Hydrogen-Bond-Mediated Folding in Depsipeptide Models of β-Turns and α-Helical Turns[1]

Elizabeth A. Gallo† and Samuel H. Gellman*

Contribution from the S. M. McElvain Laboratory of Organic Chemistry, Department of Chemistry, University of Wisconsin, 1101 University Avenue, Madison, Wisconsin 53706

Received June 14, 1993®

Abstract: The folding of several depsipeptides constructed from α-amino acids [L-proline (P) and L-alanine (A)] and α-hydroxy acids [L-lactic acid (L) and glycolic acid (G)] has been examined in methylene chloride solution by variable-temperature IR spectroscopy. Additional studies have been conducted in some cases, involving variable-temperature ^{1}H NMR spectroscopy and molecular mechanics calculations. The depsipeptides include three-residue molecules (PLL, ALL, and PLG) that can form a 13-membered-ring amide-to-amide hydrogen bond, which, for a peptide backbone, would correspond to a single turn of an α-helix. These depsipeptides can also form 10-membered-ring amide-to-ester hydrogen bonds, which would correspond to β-trun formation for a peptide backbone. For PLL and PLG, distinct N–H stretch bands can be identified for three folding patterns: non-hydrogen-bonded, β-turn, and α-helical turn. IR-based van't Hoff analyses for PLL indicate that the α-helical turn and the β-turn are both modestly enthalpically favored relative to the non-hydrogen-bonded state, but neither turn is enthalpically preferred over the other. For PLG, in contrast, the α-helical turn appears to be enthalpically preferred over both of the alternative folding patterns. Comparison between PLL and ALL indicates that the N-terminal proline residue favors α-helical turn formation. The strengths of amide-to-amide and amide-to-ester hydrogen bonds have been compared in the context of a β-turn geometry by analyzing LG and AG in CH_2Cl_2. The amide-to-amide hydrogen bond is enthalpically favored by ca. 1.6 kcal/mol, but formation of this enthalpically stronger intramolecular hydrogen bond is more costly entropically. Extrapolation from the behavior of these depsipeptides leads us to predict that for tripeptides in a nonpolar environment, a β-turn will generally be enthalpically preferred over an isolated α-helical turn. β-Turn folding has previously been widely studied in model peptides and depsipeptides; however, the present report appears to represent the first experimental effort to model formation of a single α-helical turn.

Introduction

Depsipeptides are homologues of peptides in which some of the backbone amide linkages are replaced by esters (i.e., some of the amino acid residues are replaced by hydroxy acid residues). Naturally occurring depsipeptides include the antibiotics valinomycin, beauvericin, and enniatins A, B, and C.[2] In addition to the intrinsic importance of depsipeptide conformational properties, depsipeptide folding behavior may provide insight into the behavior of the analogous peptide backbones because ester and secondary amide linkages share key structural features. Both groups are planar, by virtue of electronic resonance, and the alkyl substituent on the nitrogen or "ether" oxygen atom prefers to be syn to the carbonyl oxygen.

Conformational properties of the secondary amide and ester groups have been compared in a number of contexts. Dunitz and co-workers analyzed the geometries of amide and ester units in the crystal structures of small molecules, observing generally similar trends in the two classes.[3] Goodman et al. examined the conformational properties of polydepsipeptides and concluded that these polymers undergo helix–coil transitions qualitatively similar to those of analogous polypeptides.[4] Boussard et al. examined the folding properties of dipeptide analogues containing an ester linkage at the central position and amide "capping" groups at the N- and C-termini.[5] In nonpolar solvents, these depsipeptides display substantial intramolecular amide-to-amide hydrogen bonding in a 10-membered ring,[5] an interaction that is associated with β-turn folding patterns in peptides.[6] In the solid state, Ac-L-Pro-L-Lac-NHMe (**1**) adopts a type I β-turn conformation,[6b] which matches the β-turn preference expected for the corresponding L-Pro-L-Ala peptide sequence.[7,8]

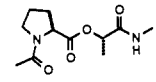

1

Secondary amides and esters differ significantly in their hydrogen-bonding properties. The secondary amide contains a hydrogen-bond donor site (the amide proton), while the ester does not. Further, the amide carbonyl is a substantially stronger hydrogen-bond acceptor than the ester carbonyl.[9] Depsipeptides are interesting compounds with which to model the local folding propensities of peptide backbones because of the combination of the ester's diminished hydrogen-bonding capability and this group's conformational similarity to the secondary amide group. We describe here the use of depsipeptide analogues of linear tripeptides to study the competition between adoption of a β-turn

* To whom correspondence should be addressed.
† Current address: Eastman Kodak Co., Research Laboratories, Building 82, Rochester, NY 14650.
® Abstract published in *Advance ACS Abstracts*, October 1, 1993.
(1) Taken in part from the Ph.D. thesis of Elizabeth A. Gallo, University of Wisconsin—Madison, 1992.
(2) Dietrich, B.; Viout, P.; Lehn, J.-M. *Macrocyclic Chemistry*; VCH: Weinheim, 1993; pp 206–215, and references therein.
(3) (a) Schweizer, W. B.; Dunitz, J. D. *Helv. Chim. Acta* **1982**, *65*, 1547. (b) Chakrabarti, P.; Dunitz, J. D. *Helv. Chim. Acta* **1982**, *65*, 1555.
(4) (a) Ingwall, R. T.; Goodman, M. *Macromolecules* **1974**, *7*, 598. (b) Becktel, W.; Wouters, G.; Simmons, D. M.; Goodman, M. *Macromolecules* **1985**, *18*, 630 and references therein.
(5) (a) Boussard, G.; Marraud, M.; Néel, J.; Maigret, B.; Aubry, A. *Biopolymers* **1977**, *16*, 1033. (b) Lecomte, C.; Aubry, A.; Protas, J.; Boussard, G.; Marraud, M. *Acta Crystallogr.* **1974**, *B30*, 1992.
(6) Rose, G. D.; Gierasch, L. M.; Smith, J. A. *Adv. Protein Chem.* **1985**, *37*, 1 and references therein.
(7) (a) Lewis, P. N.; Momany, F. A.; Scheraga, H. A. *Biochim. Biophys. Acta* **1973**, *303*, 211. (b) Chou, P. Y.; Fasman, G. D. *J. Mol. Biol.* **1977**, *115*, 135. (c) Wilmot, C. M.; Thornton, J. M. *J. Mol. Biol.* **1988**, *203*, 221.
(8) We use the terms "β-turn" and "α-helical turn" for both depsipeptides and peptides, and we consider the φ and ψ torsion angles of α-hydroxy acid residues to be analogous to the torsion angles defined for α-amino acid residues.
(9) (a) Arnett, E. M.; Mitchell, E. J.; Murty, T. S. S. R. *J. Am. Chem. Soc.* **1974**, *96*, 3875. (b) Spencer, J. N.; Garrett, R. C.; Moyer, F. J.; Merkle, J. E.; Powell, C. R.; Tran, M. T.; Berger, S. K. *Can. J. Chem.* **1980**, *58*, 1372.

0002-7863/93/1515-9774$04.00/0

Chart I

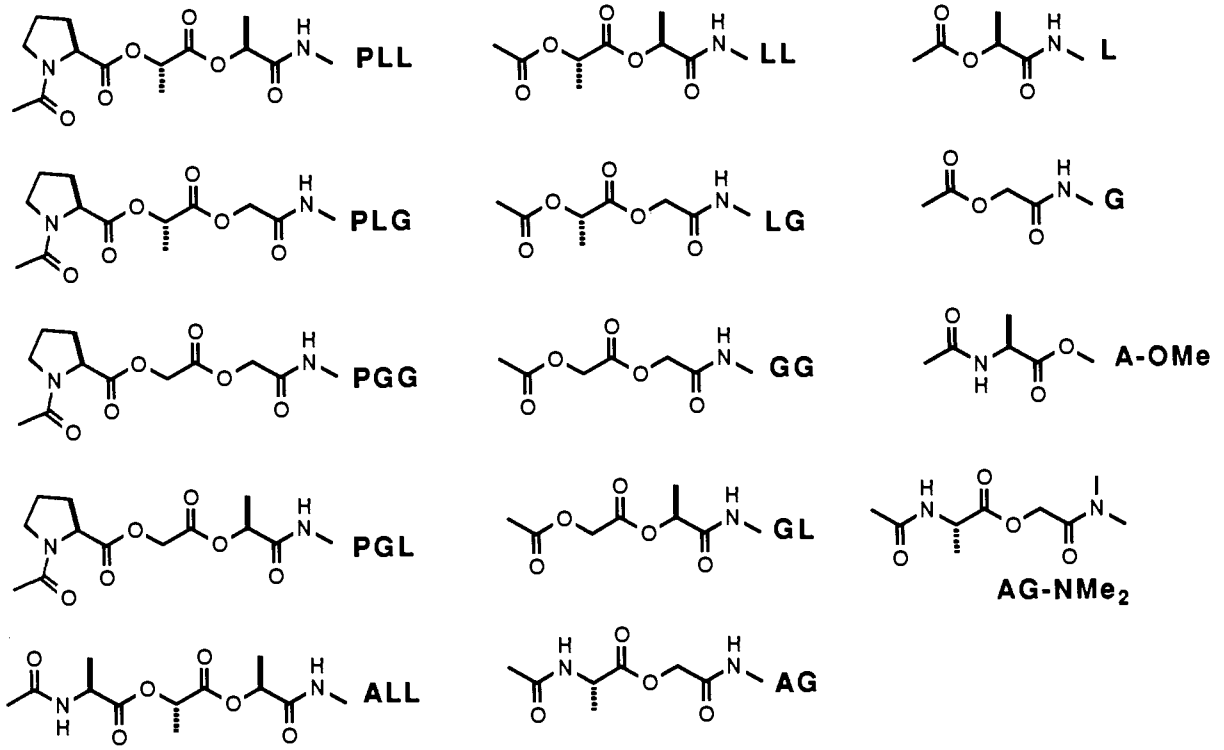

and adoption of an α-helical turn (13-membered-ring hydrogen bond). Judicious placement of amide and ester groups allows detailed IR-based analysis, including the determination of thermodynamic relationships among alternative folding patterns in some cases. The 10-membered-ring hydrogen bond associated with β-turns has been detected for many short model peptides,[6,10] but isolated α-helical turns have not received prior experimental attention to our knowledge.[11] Data on these small depsipeptides may provide insight into the way in which local conformational propensities affect protein folding patterns.

Results

Synthesis. The depsipeptides examined here are shown in Chart I, along with the one-, two-, or three-letter designations used in the text below (A for L-alanine, G for glycolic acid, L for L-lactic acid, and P for L-proline). These molecules were prepared by standard dicyclohexylcarbodiimide-mediated coupling reactions, as described in the Experimental Section. A doubling of resonances was observed in the ^{1}H NMR spectrum after final purification of each proline-containing molecule (PLL, PLG, PGL, and PGG). This resonance doubling is attributed to the occurrence of *cis–trans* isomerism about the tertiary amide C–N bond of the acetyl–proline moiety, a process that is slow on the NMR time scale.[12] The solvent dependence of the resonance ratios supported this assignment: in $CDCl_3$ and CD_2Cl_2, the species giving rise to the minor resonances typically accounted for approximately 10% of the mixture, while in DMSO-d_6, the minor species was approximately 25% of the total in each case. Previous studies have shown that the *trans* rotamer is usually predominant in small proline-containing peptides and that the proportion of the minor *cis* isomer increases in more polar solvents.[12]

Chart II

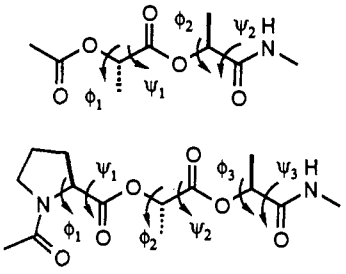

Molecular Mechanics Calculations. We carried out conformational searches with the AMBER force field[13] as implemented by MacroModel v3.0 (Multiconformer mode)[14] to gain insight into preferred conformations for intramolecularly hydrogen-bonded forms of selected depsipeptides. To evaluate β-turn preferences for LL and LG, we generated a family of starting conformations by varying each of four backbone torsion angles (ϕ and ψ for each α-hydroxy acid residue; see Chart II) by 30° increments and constraining the 10-membered-ring hydrogen-bonded O···H distance to be 0–2 Å. Minimization of the set of starting conformers for LL identified five conformations within 4 kcal/mol, all containing the 10-membered-ring hydrogen bond. The lowest energy conformation corresponded to a type I β-turn ($\phi_1 = -64°, \psi_1 = -20°, \phi_2 = -69°, \psi_2 = -17°$; ideal type I β-turn,[6] $\phi_1 = -60°, \psi_1 = -30°, \phi_2 = -90°, \psi_2 = 0°$). The next conformer was 1.0 kcal/mol higher in energy and corresponded to a type II β-turn. This conputational result suggests that the behavior of the depsipeptide backbone is similar to that of the corresponding peptide sequence, because statistical analyses of crystalline proteins

(10) For representative recent studies, see: (a) Montelione, G. T.; Arnold, E.; Meinwald, Y. C.; Stimson, E. R.; Denton, J. B.; Huang, S.-G.; Clardy, J.; Scheraga, H. A. *J. Am. Chem. Soc.* **1984**, *106*, 7984. (b) Boussard, G.; Marraud, M. *J. Am. Chem. Soc.* **1985**, *107*, 1825. (c) Wright, P. E.; Dyson, H. J.; Lerner, R. A. *Biochemistry* **1988**, *27*, 7167. (d) Falcomer, C. M.; Meinwald, Y. C.; Choudhary, I.; Talluri, S.; Milburn, P. F.; Clardy, J.; Scheraga, H. A. *J. Am. Chem. Soc.* **1992**, *114*, 4036. (e) Liang, G.-B.; Rito, C. J.; Gellman, S. H. *J. Am. Chem. Soc.* **1992**, *114*, 4440.

(11) Computational study of isolated α-helical turns: Tobias, D. J.; Brooks, C. L. *Biochemistry* **1991**, *30*, 6059.

(12) (a) Madison, V.; Schellman, J. *Biopolymers* **1970**, *9*, 511. (b) Higashijima, T.; Tasumi, M.; Miyazawa, T. *Biopolymers* **1977**, *16*, 1259.

(13) Weiner, S.; Kollman, P. A.; Nguyen, D. T.; Case, D. A. *J. Comput. Chem.* **1986**, *7*, 230.

(14) (a) Mohamdi, F.; Richards, N. G. J.; Guida, W. C.; Liskamp, R.; Lipton, M.; Caufield, C.; Chang, C.; Chang, G.; Hendrickson, T.; Still, W. C. *J. Comput. Chem.* **1990**, *11*, 440. (b) Lipton, J.; Still, W. C. *J. Comput. Chem.* **1988**, *9*, 343.

indicate that type I conformations are favored by β-turns containing alanine at positions $i + 1$ and $i + 2$ (i.e., at the second and third of the four turn residues).[8] Minimization of the starting structures for LG also generated five conformations within 4 kcal/mol. The lowest energy conformation corresponded to a type II β-turn ($\phi_1 = -67°$, $\psi_1 = +123°$, $\phi_2 = +68°$, $\psi_2 = +21°$; ideal type II β-turn,[6] $\phi_1 = -60°$, $\psi_1 = +120°$, $\phi_2 = +80°$, $\psi_2 = 0°$). The next conformer was 1.7 kcal/mol higher in energy and corresponded to a type I turn. This result further supports the conformational analogy between depsipeptide and peptide backbones, because the presence of glycine at turn residue $i + 2$ in crystalline proteins is statistically correlated with the occurrence of type II conformations.[8]

These studies were *not* intended to evaluate the relative energetics of intramolecularly hydrogen-bonded and non-hydrogen-bonded conformations, but rather to learn whether the replacement of secondary amides by esters would alter the conformations preferred when the 10-membered-ring hydrogen bond was in place. Nevertheless, it was interesting to observe that precisely the same five conformations were identified for LL when the family of starting structures was generated without including the 10-membered-ring hydrogen-bond constraint. Use of 10° torsion angle increments instead of 30° increments to generate the starting structures also did not change the low-energy conformers identified by the Multiconformer search procedure.

A conformational search was carried out for PLL to determine whether the replacement of secondary amides by esters at the turn's second and third internal residues would lead to deviation from the α-helical conformation when the 13-membered-ring hydrogen bond was in place. A family of starting structures was generated by constraining the intramolecularly hydrogen-bonded O···H distance to 0–2 Å and varying each of the lactic acid residue ϕ and ψ angles by 30° increments (ϕ_2, ψ_2, ϕ_3, and ψ_3 as defined in Chart II). The proline torsion angles (ϕ_1 and ψ_1) were held at −52° and −48° for starting structure generation; these values were obtained by minimization of PLL in a completely extended conformation. (In the final minimizations of the starting conformers, ϕ_1 and ψ_1 were not constrained.) Minimization of the family of starting conformers identified three conformations within 4 kcal/mol. The most favorable conformation corresponded to an α-helical turn ($\phi_1 = -52°$, $\psi_1 = -48°$, $\phi_2 = -67°$, $\psi_2 = -33°$, $\phi_3 = -68°$, $\psi_3 = -38°$; ideal α-helical turn,[15] $\phi_1 = -60°$, $\psi_1 = -50°$, $\phi_2 = -60°$, $\psi_2 = -50°$, $\phi_3 = -60°$, $\psi_3 = -50°$), in which all four carbonyls were approximately parallel to the hydrogen bond axis. The next conformation, 3.7 kcal/mol higher in energy, displayed a substantially different conformation, in which the two ester carbonyls were approximately perpendicular to the hydrogen bond axis. An analogous conformational search was carried out for PLG in the 13-membered-ring hydrogen-bonded form. Five conformations were identified within 4 kcal/mol, the lowest of which corresponded to an α-helical turn ($\phi_1 = -52°$, $\psi_1 = -48°$, $\phi_2 = -66°$, $\psi_2 = -34°$, $\phi_3 = -64°$, $\psi_3 = -41°$). The next conformation was 1.8 kcal/mol higher in energy. As observed for PLL, this "second best" conformation had both ester carbonyls oriented approximately perpendicular to the hydrogen bond axis.

N–H Stretch Band Assignments. Figure 1 shows N–H stretch region IR data for L, LL, and PLL, 1 mM each in CH_2Cl_2 at room temperature. The simple lactic acid derivative L shows only a single N–H stretch, at 3457 cm^{-1}, which indicates that there is no seven-membered ring (C_7) C=O···H—N hydrogen bonding under these conditions. Boussard and Marraud have previously reported a similar observation for L in CCl_4, although they detected a very small population of the C_7 form in this less

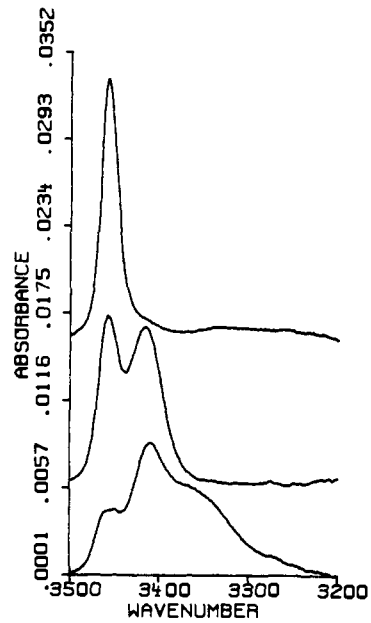

Figure 1. N–H stretch region FT-IR data for 1 mM samples of L, LL, and PLL (top to bottom) in CH_2Cl_2 at room temperature, minus the spectrum of pure CH_2Cl_2. Absorption maxima: L, 3457 cm^{-1}; LL, 3458 and 3416 cm^{-1}; PLL, 3458, 3409, and ca. 3360 cm^{-1}.

polar solvent.[16] LL shows two bands in CH_2Cl_2, at 3458 and 3416 cm^{-1}; the lower energy band must arise from intramolecular hydrogen bonding in a 10-membered ring, i.e., from β-turn formation. N–H moieties hydrogen-bonded to amide carbonyls typically give rise to bands ≤3360 cm^{-1};[17] the occurrence of the N—H···O=C(ester) band at 3416 cm^{-1} is consistent with the weaker hydrogen-bond acceptor properties of the ester carbonyl relative to the amide carbonyl. PLL shows three bands, at 3458, 3409, and ca. 3360 cm^{-1}. We assign the lowest energy band to an N–H hydrogen-bonded to an amide carbonyl, i.e., to an α-helical turn. Figure 2 shows analogous data for the G, LG, and PLG. The behavior in this series seems to be qualitatively similar to that observed for L, LL, and PLL, although the band proportions differ somewhat for the two larger members of each series.

The data for L and G demonstrate that no detectable aggregation occurs at 1 mM in CH_2Cl_2 solutions of these molecules at room temperature (intermolecular hydrogen-bonding would give rise to an absorption in the range 3420–3300 cm^{-1}). Figure 3 shows the result of an experiment designed to probe for aggregation of PLL under these conditions. There is little or no residual absorption upon subtraction of the N–H stretch spectrum obtained with a 1 mM solution (properly scaled) from the spectrum obtained with a 20 mM spectrum, indicating that even at 20 mM there is little or no aggregation of PLL in CH_2Cl_2 at room temperature.

Proline vs Alanine at the N-Terminus. Figure 4 shows N–H stretch region IR data for 1 mM solutions of A-OMe, ALL, and PLL in CH_2Cl_2 at room temperature. The spectrum for A-OMe

(15) Schulz, G. E.; Schirmer, R. H. *Principles of Protein Structure*; Springer-Verlag: New York, 1979.

(16) Boussard, G.; Marraud, M. *Biopolymers* **1981**, *20*, 169. On the basis of IR data from the ester C=O stretch region for L and related comopunds in CCl_4, these workers concluded that L experiences a weak intramolecular hydrogen bond between the amide proton and the ester group's π-system, an interaction that is not strong enough to affect the position of the N—H stretch. Ester C=O stretch data for L in CH_2Cl_2 suggest that a minor population experiences the N—H···π interaction in this more polar solvent. In this paper, we use the term "non-hydrogen-bonded" to signify the absence of an N—H···O=C(ester or amide) interaction in methylene chloride solution. Such amide protons may be involved to some extent in N—H···π interactions and/or weak dipole–dipole interactions with the solvent.

(17) For leading references on the assignment of N–H stretch bands, see: (a) Tsuboi, M.; Shimanouchi, T.; Mizushima, S. *J. Am. Chem. Soc.* **1959**, *81*, 1406. (b) Maxfield, F. R.; Leach, S. J.; Stimson, E. R.; Powers, S. P.; Scheraga, H. A. *Biopolymers* **1979**, *17*, 2507.

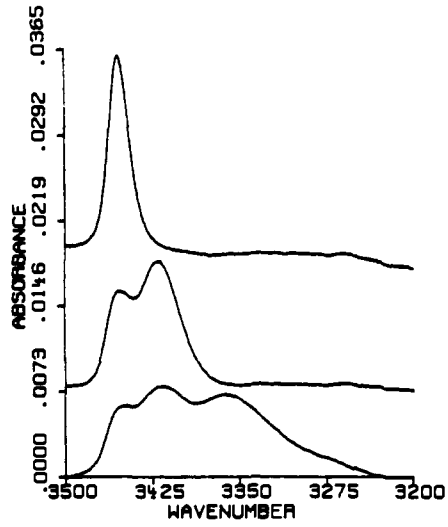

Figure 2. N–H stretch region FT-IR data for 1 mM samples of G, LG, and PLG (top to bottom) in CH_2Cl_2 at room temperature, minus the spectrum of pure CH_2Cl_2. Absorption maxima: G, 3454 cm^{-1}; LG, 3452 and 3419 cm^{-1}; PLG, 3449, 3418, and ca. 3359 cm^{-1}.

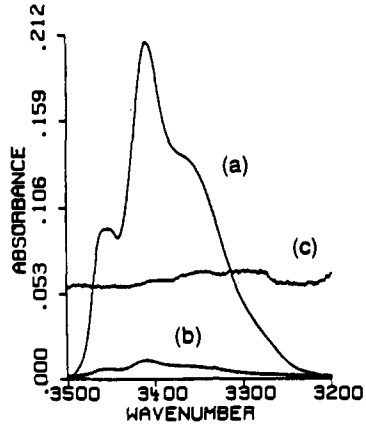

Figure 3. N–H stretch region FT-IR data for PLL in CH_2Cl_2 at room temperature, minus the spectrum of pure CH_2Cl_2: (a) 20 mM PLL; (b) 1 mM PLL; (c) spectrum shown in (a) minus the spectrum shown in (b) times 20.47.

shows a single band, at 3432 cm^{-1}. The fact that this band is 26 cm^{-1} lower in energy than the single band observed for L may be attributed to two factors: (i) branching at the saturated carbon atom adjacent to a secondary amide nitrogen causes the non-hydrogen-bonded N–H band to move to lower energy[17b,18] and (ii) there may be a C_5-type interaction between the ester carbonyl and the amide N–H of A-OMe.[5a] This latter interaction is commonly considered to be a hydrogen bond, although the large deviation of the N—H···O angle from linearity is expected to make the O···H attraction weak. ALL has two N–H moieties, but only one discrete absorbance maximum is observed in the N–H stretch region, at 3440 cm^{-1}. We attribute this somewhat broadened band to an overlap of as many as four absorptions: (i) the N-terminal N–H, affected by adjacent branching and a C_5 interaction (observed for A-OMe at 3432 cm^{-1}); (ii) the C-terminal N–H free of intramolecular hydrogen-bonding (observed for L at 3457 cm^{-1}); (iii) the C-terminal N–H engaged in a β-turn hydrogen bond (observed for LL and PLL in the range 3416–3409 cm^{-1}); and (iv) the C-terminal N–H engaged in an α-helical turn (observed for PLL at ca. 3360 cm^{-1}; this component is presumably quite small for ALL). The spectra shown in Figure 4 for PLL and ALL are displayed with the same vertical scale; since there is less absorption at 3360 cm^{-1} for ALL

(18) Boussard, G.; Marraud, M.; Aubry, A. *Biopolymers* **1979**, *18*, 1297.

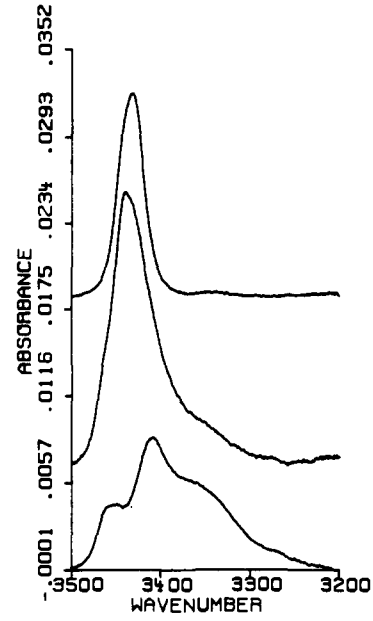

Figure 4. N–H stretch region FT-IR data for 1 mM samples of A-OMe, ALL, and PLL (top to bottom) in CH_2Cl_2 at room temperature, minus the spectrum of pure CH_2Cl_2. Absorption maxima: A-OMe, 3432 cm^{-1}; ALL, 3440 cm^{-1}; PLL, 3458, 3409, and ca. 3360 cm^{-1}.

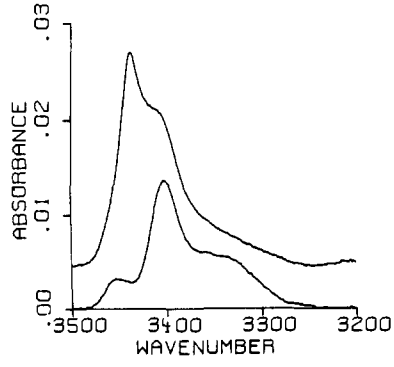

Figure 5. N–H stretch region FT-IR data for 1 mM samples of ALL (upper) and PLL (lower) in CH_2Cl_2 at 203 K, minus the spectrum of pure CH_2Cl_2 at that temperature. Absorption maxima: ALL, 3437 and 3409 cm^{-1}; PLL, 3452, 3401, and ca. 3336 cm^{-1}.

than for PLL, we conclude that the α-helical turn is less populated for ALL than for PLL under these conditions.

Figure 5 shows low-temperature N–H stretch region IR spectra for PLL and ALL, 1 mM each in CH_2Cl_2. For PLL, the three bands seen at room temperature are again observed, although the band assigned to the non-hydrogen-bonded N–H has diminished relative to the other two. For ALL, two bands are now observed, at 3437 and 3409 cm^{-1}. We assign the lower energy band to the non-hydrogen-bonded N-terminal N–H engaged in a β-turn and the higher energy band to the C-terminal N–H; this higher energy band appears to be broadened on the high-energy side, which presumably reflects the existence of some C-terminal N–H in the non-hydrogen-bonded state. Even at the low temperature, ALL shows relatively little absorption in the range 3300–3400 cm^{-1}, suggesting that there is little or no N–H hydrogen-bonded to an amide carbonyl. This observation strengthens our conclusion that an α-helical turn is less favorable for ALL than for PLL. The lack of substantial amide-to-amide hydrogen-bonding in the low temperature spectrum of ALL also indicates that there is little or no aggregation under these conditions, because we would expect intermolecular hydrogen-bonding to involve amide carbonyls as acceptors, giving rise to a band in the range 3250–3350 cm^{-1}.

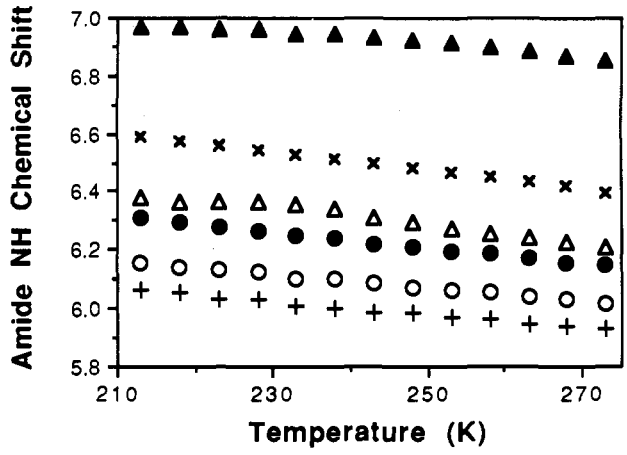

Figure 6. Temperature dependences of the amide proton ^{1}H NMR chemical shifts for 1 mM despipeptide samples in CD_2Cl_2: PLL (▲); ALL, N-terminal (×) and C-terminal N–H (+); LL (△); L (●); and A-OMe (○).

We further probed the extent of intramolecular hydrogen-bonding in ALL, PLL, and related smaller molecules by variable-temperature ^{1}H NMR spectroscopy. Figure 6 shows temperature dependences ($\Delta\delta NH/\Delta T$) of the amide proton chemical shifts for ALL, PLL, LL, L, and A-OMe, each at 1 mM in CD_2Cl_2. In contrast to the IR time scale, the NMR time scale is slow relative to equilibration among intramolecularly hydrogen-bonded and non-hydrogen-bonded states for flexible molecules. Therefore, only a single amide proton resonance is observed for each of the depsipeptides examined, even though IR spectroscopy clearly shows that at least two or three states are populated for ALL, PLL, and LL. In each case, the observed δNH is a weighted average of the contributing non-hydrogen-bonded and hydrogen-bonded states.

We have previously shown that van't Hoff $\Delta H°$ and $\Delta S°$ values can be derived for two-state folding equilibria of di- and triamides, including dipeptides, from $\Delta\delta NH/\Delta T$ data, and that these thermodynamic parameters agree well with values obtained from independent IR-based analyses.[19] Quantitative analyses of the NMR data were not attempted for the depsipeptides examined here; nevertheless, important qualitative conclusions can be drawn from the data in Figure 6. (i) β-Turn-type hydrogen-bonding involving an ester acceptor does not produce a substantial downfield shift in δNH, in contrast to the effect of intramolecular hydrogen-bonding involving an amide acceptor.[10e] This conclusion derives from the observation that δNH for LL at 273 K is only about 0.1 ppm downfield of δNH for L, even though IR data indicate that L is completely non-hydrogen-bonded and that LL is approximately 60% intramolecularly hydrogen-bonded under these conditions. (ii) PLL does, indeed, experience a greater extent of α-helical turn (amide-to-amide hydrogen-bonding) than does ALL. This conclusion is based upon the observation that δNH for PLL is 0.4–0.5 ppm downfield from the C-terminal δNH for ALL at all temperatures. (iii) ALL may experience some α-helical turn, even though there is no clear evidence in the N–H stretch region IR data, because the C-terminal δNH is ca. 0.3 ppm downfield from δNH for LL at all temperatures. (iv) The N-terminal amide proton of ALL does not appear to experience a substantial amount of intramolecular amide-to-amide hydrogen-bonding (11-membered ring, involving the C-terminal carbonyl), because this δNH is within 0.1 ppm of δNH for A-OMe at all temperatures. (v) The greater extent of α-helical turn formation in PLL relative to ALL appears to stem from an entropic advantage. This conclusion is based on the observation that the

(19) (a) Gellman, S. H.; Dado, G. P.; Liang, G.-B.; Adams, B. R. *J. Am. Chem. Soc.* **1991**, *113*, 1164. (b) Liang, G.-B.; Desper, J. M.; Gellman, S. H. *J. Am. Chem. Soc.* **1993**, *115*, 925. (c) Dado, G. P.; Gellman, S. H. *J. Am. Chem. Soc.* **1993**, *115*, 4228.

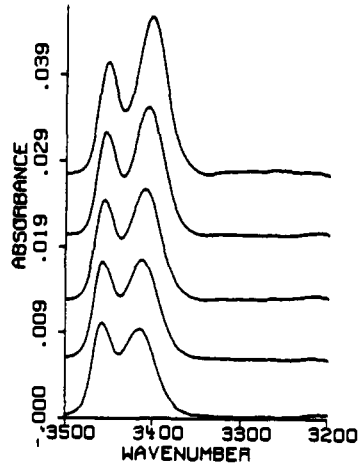

Figure 7. N–H stretch region FT-IR data for 1 mM LL in CH_2Cl_2, as a function of temperature, after subtraction of the spectrum of pure CH_2Cl_2 at the same temperature; top to bottom: 206, 234, 257, 276, and 297 K.

$\Delta\delta NH/\Delta T$ signatures for both PLL and ALL are relatively flat. δNH is a rough indicator of the equilibrium constant for the two-state equilibrium non-α-helical turn vs α-helical turn (where the former state includes non-hydrogen-bonded and β-turn hydrogen-bonded forms). According to the van't Hoff equation (eq 1), the small sensitivities of δNH to temperature suggest that

$$\ln K_{eq} = (-\Delta H°/RT) + (\Delta S°/R) \qquad (1)$$

the α-helical turn has little enthalpic advantage relative to the non-α-helical turn states for either PLL or ALL, and the increased population of the α-helical turn in PLL must result from an entropic factor.[19]

Thermodynamic Analysis. We have previously shown that thermodynamic parameters for intramolecular hydrogen-bonding equilibria of di- and triamides in chlorocarbon solvents can be obtained from variable-temperature N–H stretch region IR data.[19] Such an analysis was carried out for LL, based on the assumption that this depsipeptide's folding behavior in CH_2Cl_2 could be described in terms of two states, non-hydrogen-bonded and intramolecularly hydrogen-bonded in a β-turn (eq 2). Once the equilibrium constant for this two-state process has been determined at several temperatures, a plot of ln K_{eq} vs $1/T$ provides $\Delta H°$ and $\Delta S°$ (eq 1).

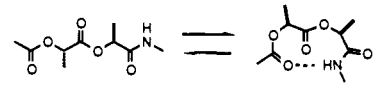

(2)

Figure 7 shows N–H stretch region data obtained for a 1 mM sample of LL at several temperatures between 203 and 297 K. Curve analysis of these spectra was carried out to estimate the "pure" constituent bands at each temperature, because the non-hydrogen-bonded and β-turn hydrogen-bonded N–H stretch bands partially overlapped (Figure 8 shows a representative curve-fitting result). Data for L obtained over the same temperature range (Figure 9) were used to define the temperature-dependent integrated extinction coefficient of the non-hydrogen-bonded N–H stretch band of LL. No model compound is available to provide an independent temperature-dependent integrated extinction coefficient for the β-turn hydrogen-bonded N–H stretch band; however, since we knew the total concentration of LL, we could determine the two-state equilibrium constant defined in eq 2 by assuming that the fraction of the total LL concentration not accounted for as non-hydrogen-bonded N–H must be in the β-turn state. Figure 10 shows a representative van't Hoff plot. Two variable-temperature IR data sets were obtained for L, and four sets were obtained for LL. Based upon the eight van't Hoff

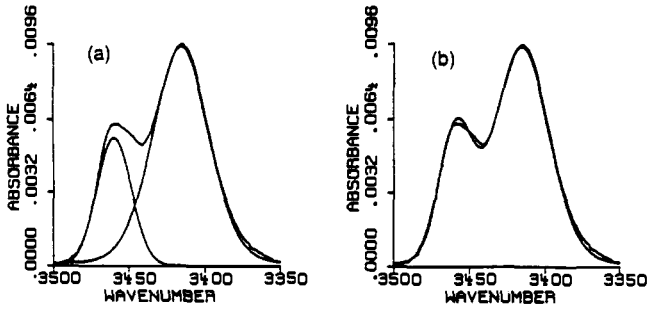

Figure 8. Representative curve-fitting result for LL, 1 mM sample in CH_2Cl_2 at 203 K, after subtraction of pure solvent: (a) individual computer-generated component bands for the non-hydrogen-bonded and β-turn hydrogen-bonded states, juxtaposed with the actual spectrum; (b) sum of the computer-generated component bands juxtaposed with the actual spectrum.

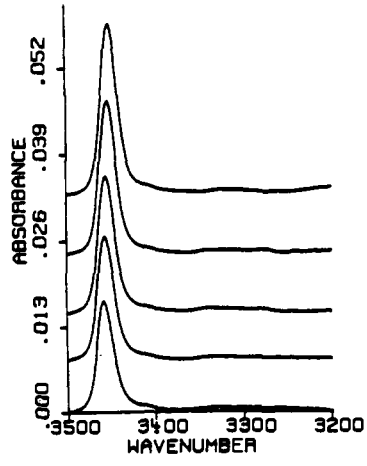

Figure 9. N–H stretch region FT-IR data for 1 mM L in CH_2Cl_2, as a function of temperature, after subtraction of the spectrum of pure CH_2Cl_2 at the same temperature; top to bottom: 204, 232, 257, 276, and 299 K.

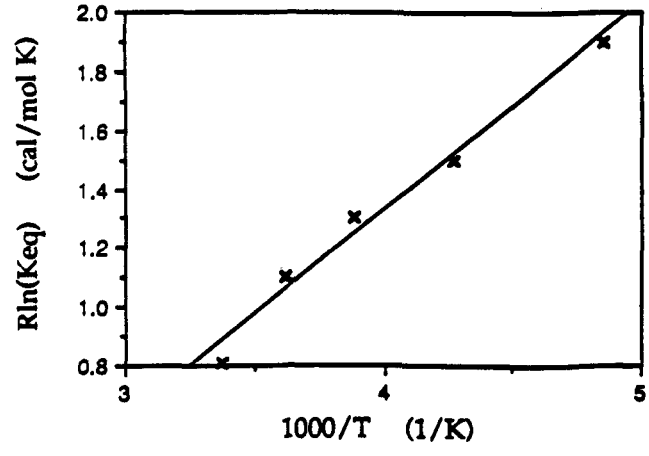

Figure 10. Representative van't Hoff plot constructed from N–H stretch region IR data for 1 mM LL in CH_2Cl_2 (data in Figure 7), based on a two-state conformational model, non-hydrogen-bonded vs β-turn, as described in the text. The line represents the best fit to equ 1, with $\Delta H°$ = –0.7 kcal/mol and $\Delta S°$ = –1 eu (correlation coefficient = 0.992).

analyses involving all possible combinations of these data sets, we conclude that the β-turn folding pattern in CH_2Cl_2 is modestly enthalpically favored relative to the non-hydrogen-bonded state ($\Delta H° = -0.6 \pm 0.2$ kcal/mol) and that the β-turn state is perhaps slightly entropically disfavored ($\Delta S° = -2 \pm 2$ eu; see Table I).

Figure 11 shows N–H stretch region IR data for a 1 mM solution of PLL in CH_2Cl_2 obtained at several temperatures between 205 and 297 K. As discussed above, the behavior of

Table I. IR-Based Thermodynamic Parameters for Non-Hydrogen-Bonded vs β-Turn States of Depsipeptides LL, LG, and AG in CH_2Cl_2

dipsipeptide	$\Delta H°$ (kcal/mol)	$\Delta S°$ (eu)
LL	–0.6 ± 0.2	–2 ± 2
LG	–0.4 ± 0.1	–0.3 ± 0.5
AG	–2.0 ± 0.2	–4 ± 1

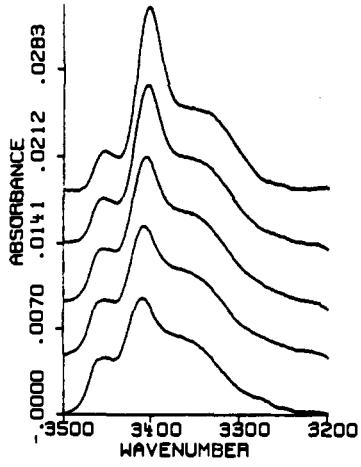

Figure 11. N–H stretch region FT-IR data for 1 mM PLL in CH_2Cl_2, as a function of temperature, after subtraction of the spectrum of pure CH_2Cl_2 at the same temperature; top to bottom: 204, 232, 257, 276, and 299 K.

PLL under these conditions is best described in terms of three states: non-hydrogen-bonded, β-turn, and α-helical turn. Figure 12 shows the mathematical decomposition of a representative N–H stretch region spectrum into bands corresponding to these three states. We used the temperature-dependent integrated extinction coefficient provided by the variable-temperature N–H stretch data for L (Figure 9) to determine the population of the non-hydrogen-bonded state of PLL. To determine the β-turn state population, we used the temperature-dependent integrated extinction coefficient implied for the appropriate N–H stretch band by our analysis of LL. The population of the α-helical state was then assumed to be that fraction of the total PLL concentration not accounted for by the sum of the non-ydrogen-bonded and β-turn states.

Two different van't Hoff analyses were carried out for PLL, based on each of the two-state equilibrium constants defined in eqs 3 and 4. Equation 3 describes the equilibrium as non-β-turn

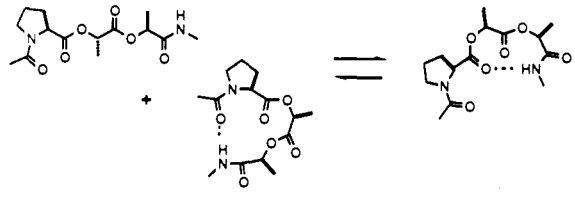

(3)

vs β-turn, where the non-β-turn state comprises non-hydrogen-bonded and α-helical turn forms. Equation 4 describes the equilibrium as non-α-helical turn vs α-helical turn, where the non-α-helical turn-state comprises non-hydrogen-bonded and β-turn forms. Representative van't Hoff plots based on eqs 3 and

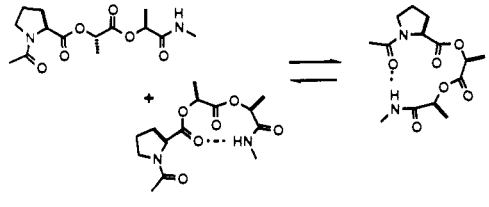

(4)

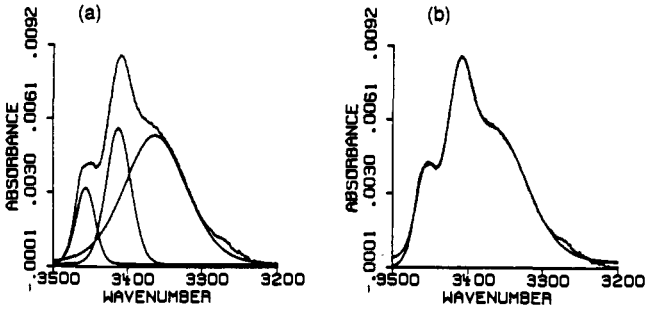

Figure 12. Representative curve-ftting result for PLL, 1 mM sample in CH_2Cl_2 at 207 K, after subtraction of pure solvent: (a) individual computer-generated component bands for the non-hydrogen bonded, β-turn hydrogen-bonded, and α-helical turn hydrogen-bonded states, juxtaposed with the actual spectrum; (b) sum of the computer-generated component bands juxtaposed with the actual spectrum.

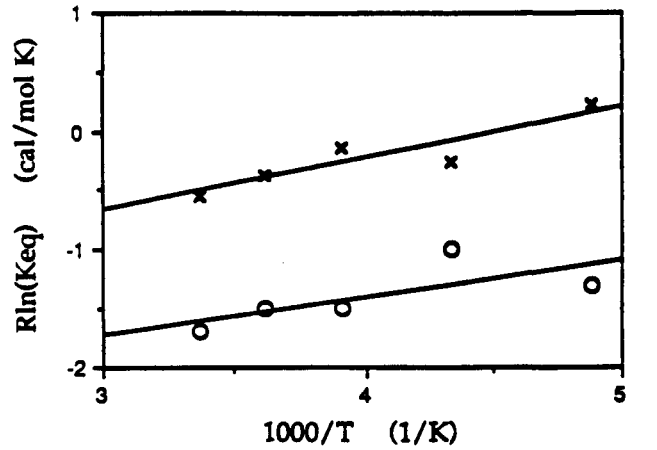

Figure 13. Representative van't Hoff plots constructed from N–H stretch region IR data for 1 mM PLL in CH_2Cl_2 (data in Figure 11), as described in the text. (×) Analysis based on the two-state conformational model non-β-turn vs β-turn, eq 3; the line represents the best fit to eq 1, with $\Delta H^\circ = -0.4$ kcal/mol and $\Delta S^\circ = -2$ eu (correlation coefficient = 0.919). (○) Analysis based on the two-state conformational model non-α-helical turn vs α-helical turn, eq 4; the line represents the best fit to eq 1, with $\Delta H^\circ = -0.3$ kcal/mol and $\Delta S^\circ = -3$ eu (correlation coefficient = 0.720).

Table II. IR-Based Thermodynamic Parameters for Non-β-Turn vs β-Turn and for Non-α-Helical Turn vs α-Helic Turn, as Defined in the Text, Depsipeptides PLL and PLG

depsipeptide	$\Delta H^\circ, \beta$ (kcal/mol)[a]	ΔS°, β (eu)[a]	$\Delta H^\circ, \alpha$ (kcal/mol)[b]	ΔS°, α (eu)[b]
PLL	−0.5 ± 0.2	−3 ± 1	−0.4 ± −.1	−3 ± 1
PLG	+0.3 ± 0.1	−1 ± 1	−0.8 ± 0.1	−3 ± 1

[a] Non-β-turn vs β-turn as defined in eq 3 for PLL and eq 7 for PLG. [b] Non-α-helical turn vs α-helical turn as defined in eq 4 for PLL and eq 8 for PLG.

4 are shown in Figure 13. Analyses were carried out using all 12 possible combinations among one data set for L, four data sets for LL, and three data sets for PLL (summarized in Table II). The results indicate that both the β-turn and the α-helical turn are modestly enthalpically favored relative to the composite alternative states ($\Delta H^\circ = -0.5 \pm 0.2$ and -0.4 ± 0.1 kcal/mol, respectively, for eqs 3 and 4) and that each of these folded states is modestly entropically disfavored ($\Delta S^\circ = -3 \pm 1$ eu in each case). Thus, the thermodynamic favorability of the α-helical turn and β-turn states of PLL in CH_2Cl_2 seems to be nearly identical.

To examine the conformational effect of removing one of the depsipeptide's side-chain methyl groups, β-turn formation was evaluated for LG by a procedure analogous to that described above for LL. Figure 14 shows N–H stretch region data obtained with a 1 mM sample of LG in CH_2Cl_2 between 204 and 299 K.

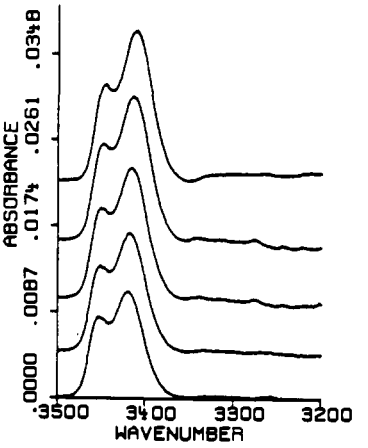

Figure 14. N–H stretch region FT-IR data for 1 mM LG in CH_2Cl_2, as a function of temperature, after subtraction of the spectrum of pure CH_2Cl_2 at the same temperature; top to bottom: 204, 231, 255, 276, and 299 K.

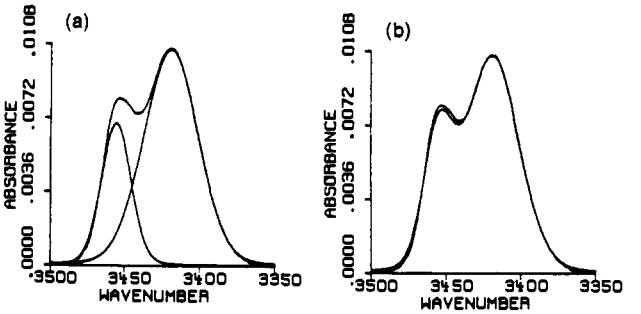

Figure 15. Representation curve-fitting result for LG, 1 mM sample in CH_2Cl_2 at 205 K, after subtraction of pure solvent: (a) individual computer-generated component bands for the non-hydrogen-bonded and β-turn hydrogen-bonded states, juxtaposed with the actual spectrum; (b) sum of the computer-generated component bands juxtaposed with the actual spectrum.

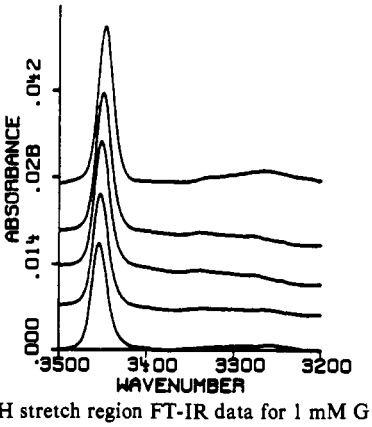

Figure 16. N–H stretch region FT-IR data for 1 mM G in CH_2Cl_2, as a function of temperature, after subtraction of the spectrum of pure CH_2Cl_2 at the same temperature; top to bottom: 204, 231, 255, 276, and 299 K.

Mathematical decomposition of these spectra allowed us to approximate the absorbances corresponding to the non-hydrogen-bonded and β-turn states (Figure 15). The temperature-dependent integrated extinction for the non-hydrogen-bonded band was estimated from variable-temperature data for G (Figure 16). Six van't Hoff analyses were carried out based on the two-state equilibrium shown in eq 5, using all combinations of two

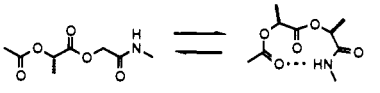

(5)

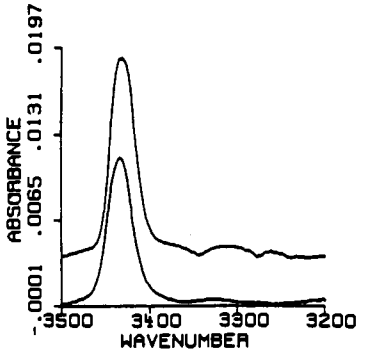

Figure 17. N–H stretch region FT-IR data for 1 mM AG-NMe_2 in CH_2Cl_2, after subtraction of the spectrum of pure CH_2Cl_2, at 207 K (upper) and 295 K (lower; absorption maximum at 3433 cm^{-1}).

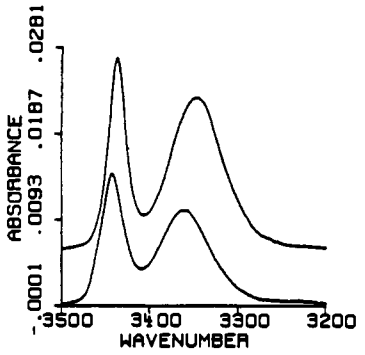

Figure 18. N–H stretch region FT-IR data for 1 mM AG in CH_2Cl_2, after subtraction of the spectrum of pure CH_2Cl_2, at 205 K (upper) and 295 K (lower; absorption maxima at 3442 and 3360 cm^{-1}).

data sets for G and three data sets for LG. These analyses indicated that β-turn formation is modestly enthalpically favored ($\Delta H° = -0.4 \pm 0.1$ kcal/mol) and entropically neutral ($\Delta S° = -0.3 \pm 0.5$ eu) in CH_2Cl_2 (Table I).

We examined folding thermodynamics for AG to determine the effect of replacing the ester hydrogen-bond acceptor of LG with an amide. As a preliminary control, we also studied AG-NMe_2. Figure 17 shows variable-temperature IR data for a 1 mM CH_2Cl_2 solution of AG-NMe_2. Only one N–H stretch band is observed, at 3433 cm^{-1}, which is similar to the lone N–H stretch band seen for A-OMe (Figure 4). The behavior of AG-NMe_2 shows that amide-to-amide hydrogen-bonding in an eight-membered ring, a possible alternative to β-turn formation in AG, does not occur. The data in Figure 17 also indicate that intermolecular hydrogen-bonding is not significant in a 1 mM sample, even at the lowest temperatures examined.

Figure 18 shows N–H stretch region IR data for a 1 mM sample of AG in CH_2Cl_2 at 205 and 295 K. The band at 3360 cm^{-1} is assigned to the C-terminal N–H moiety engaged in a β-turn hydrogen bond. As expected, this hydrogen-bonded band is significantly lower in energy than the analogous amide-to-ester hydrogen-bonded N–H stretch band in LG (3419 cm^{-1}; see Figure 14), reflecting the stronger hydrogen-bond-accepting properties of the amide relative to the ester. The higher energy band in Figure 18, at 3442 cm^{-1}, presumably arises from the completely non-hydrogen-bonded N-terminal N–H and from the non-hydrogen-bonded population of the C-terminal N–H. To try to resolve these non-hydrogen-bonded bands, we prepared ^{15}N-AG, in which the N-terminal N–H was isotopically labeled with nitrogen-15. This isotopic labeling is expected to lower the ^{15}N-H stretch band by ca. 12 cm^{-1}, relative to the position for the naturally predominant ^{14}N–H.[20] Figure 19 shows an N–H stretch region IR spectrum of 1 mM ^{15}N-AG in CH_2Cl_2 along with the results of curve fitting, which indicates the presence of two high-energy N–H stretch bands. The minor component at 3456 cm^{-1} is assigned to the non-hydrogen-bonded population of

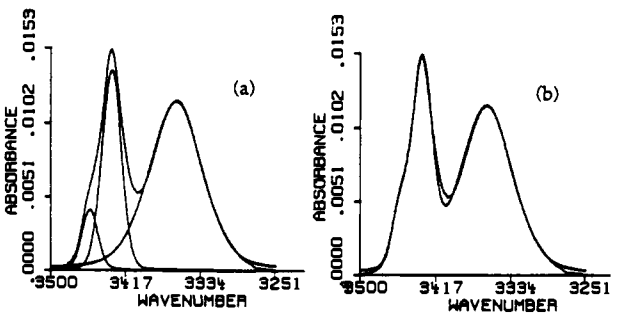

Figure 19. Representative curve-fitting result for ^{15}N-AG, 1 mM sample in CH_2Cl_2 at 294 K, after subtraction of pure solvent: (a) individual computer-generated component bands for the non-hydrogen-bonded C-terminal ^{14}N–H, the non-hydrogen-bonded N-terminal ^{15}N–H, and the β-turn hydrogen-bonded C-terminal ^{14}N–H, juxtaposed with the actual spectrum; (b) sum of the computer-generated component bands juxtaposed with the actual spectrum.

the C-terminal N–H, based on the observation that G shows only a single N–H stretch band at 3454 cm^{-1}. The major component at 3433 cm^{-1} is assigned to the N-terminal ^{15}N–H.

The assignment of the 3433 cm^{-1} band of ^{15}N-AG to the N-terminal N–H requires some comment. Since the ^{15}N substitution should cause a ca. 12-cm^{-1} decrease in band position,[20] we expect the non-hydrogen-bonded N-terminal N–H stretch band in unlabeled AG to occur at ca. 3445 cm^{-1} (indeed, the single non-hydrogen-bonded N–H stretch maximum seen for AG in Figure 18 occurs at 3442 cm^{-1}). Why should this band occur >10 cm^{-1} higher than the analogous bands of A-OMe and AG-NMe_2 (Figures 4 and 17)? In discussing A-OMe, we noted that the N–H moiety of this molecule has been proposed to engage in a C_5 interaction with the ester carbonyl.[5a] Formation of a β-turn precludes this C_5 interaction. Since the spectral decomposition shown in Figure 19 indicates AG-NMe_2 to be largely in the β-turn state, we expect little or none of the N-terminal N–H to be engaged in a C_5 interaction. Therefore, we conclude that the C_5 interaction involving an ester carbonyl causes a 12–13-cm^{-1} shift to lower energy in the stretch bands for the N–H moieties of A-OMe and AG-NMe_2 relative to the N-terminal N–H of AG.

Figure 20 shows N–H stretch region data obtained between 205 and 294 K for 1 mM ^{15}N-AG in CH_2Cl_2. van't Hoff analysis

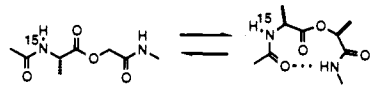

(6)

was carried out on the basis of the two-state folding hypothesis embodied in eq 6. The temperature-dependent integrated extinction coefficient determined for the lone N–H stretch band of G (Figure 16) was used to determine the concentration of the non-β-turn state for ^{15}N-AG, based on the higher energy non-hydrogen-bonded N–H stretch band in Figure 20. That portion of the total depsipeptide concentration not accounted for as non-β-turn was assumed to be in the β-turn state. Based upon calculations involving all four combinations of two IR data sets for G and two data sets for ^{15}N-AG, we conclude that β-turn formation in methylene chloride is quite enthalpically favorable

(20) For a localized A–B stretch, the band position can be estimated from the equation

$$\nu = (2\pi c)^{-1}[k(M_A + M_B)/M_A M_B]^{1/2}$$

where c is the speed of light, k is the force constant of the A–B bond, M_A is the mass of atom A, and M_B is the mass of atom B. (See, for example: Silverstein, R. M.; Bassler, G. C.; Morrill, T. C. *Spectrometric Identification of Organic Compounds*, 5th Ed.; John Wiley & Sons: New York, 1991; p 93). This type of calculation predicts a ^{15}N–H stretch to occur ca. 12 cm^{-1} lower in energy than a ^{14}N–H stretch.

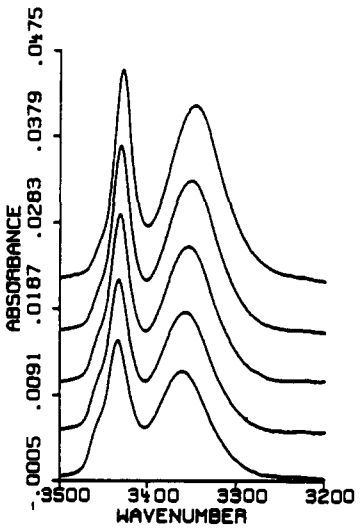

Figure 20. N–H stretch region FT-IR data for 1 mM ^{15}N-AG in CH_2Cl_2, as a function of temperature, after subtraction of the spectrum of pure CH_2Cl_2 at the same temperature; top to bottom: 205, 233, 255, 275, and 294 K.

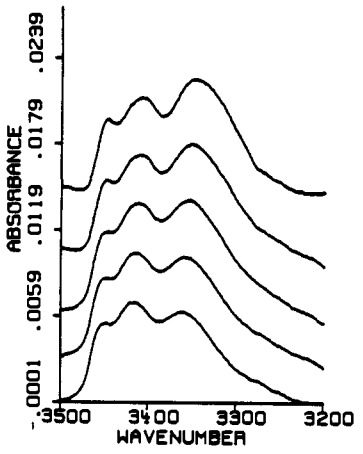

Figure 21. N–H stretch region FT-IR data for 1 mM PLG in CH_2Cl_2, as a function of temperature, after subtraction of the spectrum of pure CH_2Cl_2 at the same temperature; top to bottom: 207, 231, 257, 277, and 298 K.

($\Delta H°$ = –2.0 ± 0.2 kcal/mol) but moderately entropically unfavorable ($\Delta S°$ = –4 ± 1 eu). These findings are summarized in Table I.

Figure 21 shows N–H stretch region IR data obtained for a 1 mM sample of PLG in CH_2Cl_2 between 207 and 298 K. Figure 22 shows a representative mathematical decomposition of a three-component PLG N–H spectrum. Thermodynamic analysis was conducted as described for PLL: the non-hydrogen-bonded and β-turn populations were determined using integrated extinction coefficients obtained from data for G and LG, and the α-helical turn population was assumed to be that portion of the total depsipeptide concentration not accounted for by the other two states. van't Hoff analyses were carried out on the basis of each of the two-state scenarios indicated graphically below, non-β-turn vs β-turn (eq 7) and non-α-helical turn vs α-helical turn (eq 8). The results, summarized in Table I, indicate that β-turn formation is slightly disfavored enthalpically ($\Delta H°$ = +0.3 ± 0.1 kcal/mol) and approximately neutral entropically ($\Delta S°$ = –1 ± 1 eu and that α-helical turn formation is significantly favored enthalpically ($\Delta H°$ = –0.8 ± 0.1 kcal/mol) and somewhat entropically disfavored ($\Delta S°$ = –3 ± 1 eu).

Sources of Quantitative Error. The IR measurements underlying the thermodynamic analyses for LL, LG, AG, PLL, and PLG were quite reproducible, as were the results of computer-based recontruction of the IR spectra via curve-fitting procedures. (In contrast, curve-fitting analysis was unsuccessful for related depsipeptides GL, GG, PGL, and PGG; these molecules were prepared to complete a homologous series in which methyl group side chains were systematically removed.) In previous studies of intramolecular hydrogen-bonding equilibria, we have evaluated the significance of possible systematic errors inherent in the IR-based analysis by carrying out independent NMR-based determinations of van't Hoff $\Delta H°$ and $\Delta S°$.[19] For several diamides containing only one N–H moiety and for which the non-hydrogen-bonded and intramolecularly hydrogen-bonded N–H stretch bands were well resolved, we have found good agreement between $\Delta H°$ and $\Delta S°$ values derived from variable-temperature IR and ^{1}H NMR measurements. We have also compared IR- and NMR-based analyses for two triamides containing two N–H moieties (*N*-malonyl alanine derivative **2**[19c] and Ac-L-Pro-L-Ala-NHMe (**3**)[21]), systems that required spectral deconvolution/curve-fitting protocols similar to the one employed here. In both of these cases, the agreement between $\Delta H°$ values obtained from IR and NMR methods was good, but the agreement between $\Delta S°$ values was poorer, with the IR-based analyses yielding $\Delta S°$ values about half as large as those from the NMR-based analyses (–3.3 vs –6.4 eu for **2**,[19c] –2.8 vs –5.3 eu for **3**[21]). $\Delta S°$ is obtained from the vertical axis intercept in a van't Hoff plot, while $\Delta H°$ is obtained from the slope; therefore, $\Delta S°$ is particularly sensitive to errors arising from inaccuracies in the absolute concentrations of the states in equilibrium. Based on these prior findings, we believe that the IR-based $\Delta H°$ values we have determined for depsipeptide folding in CH_2Cl_2 are reasonably accurate but that

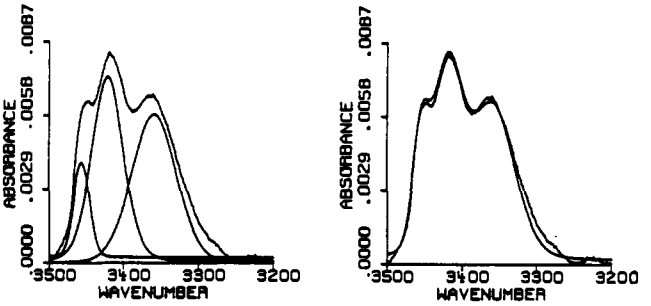

Figure 22. Representative curve-fitting result for PLG, 1 mM sample in CH_2Cl_2 at 298 K, after subtraction of pure solvent: (a) individual computer-generated component bands for the non-hydrogen-bonded, β-turn hydrogen-bonded, and α-helical turn hydrogen-bonded states, juxtaposed with the actual spectrum; (b) sum of the computer-generated component bands juxtaposed with the actual spectrum.

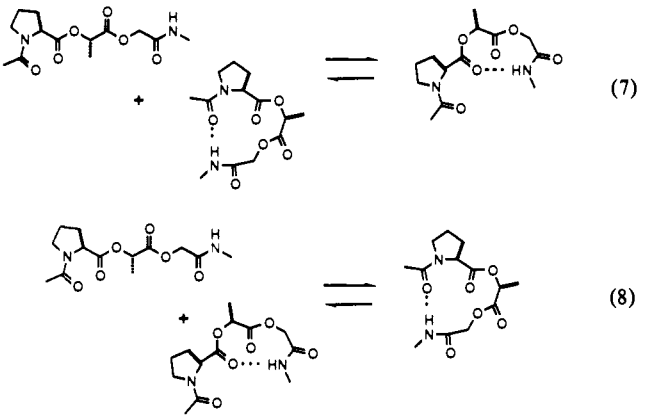

(7)

(8)

(21) Liang, G.-B., Ph.D. Thesis, University of Wisconsin—Madison, 1992.

the $\Delta S°$ values may be too small by as much as a factor of 2. This uncertainty does not affect the qualitative conclusions presented below.

There is an additional source of potential systematic error for the proline-containing depsipeptides. As discussed above, ^1H NMR spectra of PLL and PLG in CD_2Cl_2 reveals the presence of approximately 10% of the *cis* proline rotamer. Molecular modeling suggests that formation of the 13-membered-ring hydrogen bond is considerably less favorable in this rotamer than in the predominant *trans* rotamer.[22] Therefore, the non-hydrogen-bonded N–H stretch band observed for PLL in Figure 11 and for PLG in Figure 21 probably arises in part from this *cis* rotamer. The N–H stretch band arising from the β-turn should also contain a contribution from the *cis* rotamer, but the N–H stretch band assigned to the α-helical turn is likely to arise largely or exclusively from the *trans* rotamer. To estimate the maximum effect of this minor *cis* rotamer population on the derived $\Delta H°$ and $\Delta S°$ values for α-helical taurn formation, we carried out modified van't Hoff analyses for PLL and PLG, based on IR data shown in Figures 11 and 21. These IR data were obtained with 1 mM depsipeptide solutions; in the modified analyses, the population of the non-α-helical turn states defined in eqs 4 and 8 were reduced by 0.1 mM at each temperature, and new van't Hoff plots were constructed. The resulting $\Delta H°$ and $\Delta S°$ values were within the uncertainties given in Table II. If the minor *cis* rotamer experienced some 13-membered-ring hydrogen-bonding, then the effect on the derived $\Delta H°$ and $\Delta S°$ values would be even smaller. The effect of a *cis* correction on β-turn $\Delta H°$ and $\Delta S°$ values should also be small, because the *cis* rotamer presumably contributes to both the β-turn and non-β-turn states. Based on these results, we conclude that the presence of the minor *cis* rotamers of PLL and PLG does not significantly affect the thermodynamic parameters we have obtained from van't Hoff analysis.

Discussion

Depsipeptides as Conformational Models for Peptides. As indicated in the Introduction, several prior studies have suggested that the conformational properties of ester and secondary amide groups are similar, particularly in molecules containing α-hydroxy acid residues in place of α-amino acid residues. Boussard et al. have shown that dipeptide analogues containing an ester linkage at the central position from β-turn-like 10-membered-ring hydrogen bonds between the terminal amide groups.[5] Most of the dipeptide analogues we examined contained two ester groups, at the central position and at the end corresponding to the N-terminus. In these caess, the β-turn-like hydrogen bond involves an ester carbonyl as acceptor. Before examining these molecules experimentally, we employed a molecular mechanics method to explore the conformational preferences of the 10-membered hydrogen-bonded ring in these depsipeptides. For both LL and LG, results of the Multiconformer searches were consistent with the β-turn preferences expected for the corresponding peptide sequences.

The principal goal of these computational studies was to evaluate alternative conformations for the intramolecularly hydrogen-bonded ring. We did not expect the AMBER/MacroModel v3.0 approach to be suitable for evaluating the relative energetics of intramolecularly hydrogen-bonded and non-hydrogen-bonded conformations (i.e., β-turn vs extended conformations), because such calculations have been shown to overestimate the energetic significance of intramolecular hydrogen bonds.[23] Such overestimation is expected to be particularly acute for calculations carried out with isolated molecules, as in the present case, but the problem arises even when an effort is made to account for the effects of a low-polarity solvent.[23] When we carried out a conformational search for an isolated molecule of LL starting from an extended conformation, only intramolecularly hydrogen-bonded conformations were identified within 4 kcal/mol of the type I β-turn. This *in vacuo* computational result contrasts with our experimental observation that the β-turn state of LL is enthalpically favored relative to the non-hydrogen-bonded state by <1 kcal/mol in CH_2Cl_2.

For both PLL and PLG, the lowest energy conformation of the 13-membered hydrogen-bonded ring identified by a Multiconformer search corresponded to an α-helical sequence of torsion angles. Non-α-helical conformations of the 13-membered hydrogen-bonded ring were considerably higher in energy. These findings suggest that the amide-to-amide hydrogen-bonding detected by IR for PLL and PLG does, indeed, correspond to an α-helical turn.

Hydrogen-Bond-Driven Folding. The type of model study we have described pits the enthalpic gain of intramolecular hydrogen bond formation against several forces that oppose the adoption of compact conformations: torsional strain, conformational entropy, and any unfavorable dipolar interactions that develop in particular folding patterns. Thermodynamic data from this type of study provide insight into the way in which local interactions influence the conformational preferences of the depsipeptide backbone under scrutiny. Our data should also be relevant to the β-turn and α-helical turn preferences of peptide backbones, because of the expected parallels between depsipeptide and peptide conformational behavior.

Intramolecular hydrogen bonds serve a second role in our study: in addition to providing a driving force for folding, the hydrogen bonds provide a spectroscopic handle that allows detection of and discrimination among folded states. Nonpolar solvents must be employed if folding equilibria are to be evaluated in very small peptides and depsipeptides (1–3 residues), because polar solvents (e.g., water) disrupt intramolecular hydrogen bonds, and therefore folding, in molecules of this size. The use of nonpolar solvents in studies ultimately aimed at elucidating protein folding behavior is sometimes criticized on the ground that proteins themselves fold in aqueous solution; thus, the argument runs, only model studies carried out in aqueous solution are biologically relevant. We believe that this argument is overly simplistic. Many proteins adopt their native structures in membranes, the interiors of which are nonpolar. Among proteins that fold in aqueous solution, most of the intramolecular hydrogen bonds are buried away from the aqueous medium, according to crystallographic analysis.[24] The dielectric constant that characterizes interior regions of proteins is still a subject of debate, and will no doubt vary from case to case, but it seems to be agreed that interior regions often have considerably lower dielectric constants than bulk aqueous solution.[25] In such interior regions, therefore, the enthalpic penalty for breaking an intramolecular hydrogen bond will be greater than in aqueous solution, where surrounding water molecules can accommodate unpaired donor or acceptor groups. No solvent can perfectly reproduce the "typical" protein interior microenvironment, but water is clearly *not* a valid choice for modeling these interior regions.

(22) To assess the favorability of 13-membered-ring hydrogen-bonding in the *cis* proline rotamer of PLL, we carried out Multiconformer searches (AMBER/MacroModel v3.0) with this rotamer. These searches identified folded conformations containing the 13-membered-ring hydrogen bond that were >4 kcal/mol higher in energy than the α-helical turn conformation of the *trans* proline rotamer; however, we cannot be certain that the *cis* rotamer searches identified the most favorable conformation containing a 13-membered hydrogen bond.

(23) Gellman, S. H.; Dado, G. P. *Tetrahedron Lett.* **1991**, *32*, 7737 and references therein. It has recently been shown that reparametrization of AMBER using the results of high-level ab initio calculations leads to a force field (AMBER*) that treats intramolecular hydrogen-bonding in small oligoamides more realistically: McDonald, D. Q.; Still, W. C. *Tetrahedron Lett.* **1992**, *33*, 7743,7747.

(24) Baker, E. N.; Hubbard, R. E. *Prog. Biophys. Molec. Biol.* **1984**, *44*, 97.

(25) For leading references, see: (a) Dill, K. A. *Biochemistry* **1990**, *29*, 7133. (b) Gilson, M. K.; Honig, B. H. *Nature* **1987**, *330*, 84. (c) Rodgers, K. K.; Sligar, S. G. *J. Am. Chem. Soc.* **1991**, *113*, 9419.

In contrast to the large number of studies on β-turn formation in short peptides,[5,6,10] there has been no prior experimental examination of isolated α-helical turns in solution to our knowledge.[11] For a first effort in this area, we decided to bias the system toward the α-helical turn, relative to competing β-turns, by replacing the two internal amide linkages of a tripeptide with esters. These replacements eliminate the β-turn involving the N-terminal amide carbonyl as acceptor, because the corresponding donor group is missing, and these replacements discriminate against the β-turn involving the C-terminal amide N–H as a donor by making the corresponding hydrogen-bond acceptor an ester carbonyl. Even with this bias, the latter β-turn provides stiff competition in the folding equilibrium. At room temperature in CH_2Cl_2, approximately 27% of PLL is non-hydrogen-bonded, 43% is in the β-turn state, and 30% is in the α-helical turn state. For PLG, the approximate populations are 23%, 25%, and 52%.

The ability of the β-turn (amide-to-ester hydrogen bond) to compete effectively with the α-helical turn (amide-to-amide hydrogen bond) prompted us to carry out a direct comparison of these two types of hydrogen bonds as driving forces for adoption of a β-turn folding pattern. Thermodynamic results for LG and AG (Table I) indicate that the amide-to-amide hydrogen-bonded folding pattern is ca. 1.6 kcal/mol more stable enthalpically than the analogous amide-to-ester hydrogen-bonded folding pattern. For a given hydrogen-bonded ring closure equilibrium, the $\Delta H°$ value is not equal to the hydrogen bond strength, because other factors (e.g., torsional strain and steric repulsions present in the folded but not in the unfolded state) contribute to the total folding enthalpy. $\Delta\Delta H°$ for AG vs LG, however, should correspond closely to the difference between amide-to-amide and amide-to-ester hydrogen bonds in the type II β-turn geometry, since most other enthalpic contributions should be similar in the two cases.

Our $\Delta\Delta H°$ value of ca. 1.6 kcal/mol for amide-to-amide vs ester-to-amide hydrogen bonds in the β-turn geometry can be compared to literature data for *intermolecular* hydrogen bonds involving amide and ester carbonyls. Arnett et al. calorimetrically measured hydrogen bond enthalpies between *p*-fluorophenol and a large number of hydrogen-bond acceptors, including ethyl acetate (–4.7 kcal/mol), *N*,*N*-dimethylacetamide (–7.4 kcal/mol), *N*-methylformamide (–6.4 kcal/mol), and *N*,*N*-dimethylformamide (–7.0 kcal/mol).[9a] Spencer et al. calorimetrically determined the enthalpies of hydrogen-bond donation from *N*-methylacetamide to ethyl acetate (–2.9 kcal/mol) and to *N*,*N*-dimethylacetamide (–3.9 kcal/mol) and from *N*-methylformamide to ethyl acetate (–2.3 kcal/mol) and to *N*,*N*-dimethylacetamide (–3.1 kcal/mol).[9b] The trends from both studies are qualitatively consistent with our observation that the amide-to-ester hydrogen bond is enthalpically weaker than the amide-to-amide hydrogen bond, although our $\Delta\Delta H°$ value is somewhat larger than the differences in intermolecular hydrogen bond enthalpies reported by Spencer et al.[9b] The intriguing observation that hydrogen-bonded ring closure is more *entropically* costly for AG than for LG may indicate that the geometric preferences for the amide-to-amide hydrogen bond are more stringent than those for the amide-to-ester hydrogen bond.

Comparison of the α-helical turn and β-turn $\Delta H°$ and $\Delta S°$ values for PLL, PLG, and AG (Tables I and II) suggests that the α-helical turn would be populated to a much lower extent in the three-residue molecules if the competing β-turn involved amide-to-amide rather than amide-to-ester hydrogen bond formation. By extention, it seems likely that a β-turn would be generally preferred over an isolated α-helical turn for peptide backbones as well. This conclusion is consistent with the observation that isolated α-helical turns are relatively rare in crystalline proteins,[25a] while isolated β-turns are quite common.[6,7] Our data imply that for peptide backbones, formation of a single α-helical turn is less favorable *enthalpically* than β-turn formation in nonpolar environments. This conclusion is interesting, since an amide-to-amide hydrogen bond would be formed in each case. The apparent enthalpic inferiority of the α-helical turn may reflect, at least in part, the necessity of aligning four amide dipoles (i.e., the hydrogen-bond donor and acceptor and those of the two intervening peptide linkages). In contrast, only the hydrogen-bond donor and acceptor groups' dipoles are aligned in the β-turn conformation.

α-Helical Turn Formation: PLL vs PLG. One surprising result of this study is the difference in the folding thermodynamics of PLL and PLG (Table II). For PLL in CH_2Cl_2, the β-turn and α-helical turn states are each modestly enthalpically preferred and entropically disfavored relative to the composite alternative state consisting of the other turn and non-hydrogen-bonded forms. In terms of both $\Delta H°$ and $\Delta S°$, the β-turn and α-helical turn states of PLL seem to be closely matched. For PLG, in contrast, the α-helical turn state is substantially more favorable enthalpically but also more costly entropically than the β-turn state. Comparison between LL and LG (Table I) indicates that the β-turn folding patterns available to these two segments have similar absolute enthalpic favorabilities; therefore, the variation in folding enthalpies between PLG and PLL appears to reflect a difference in α-helical turn propensities. The difference in α-helical turn $\Delta H°$ values probably arises from differences in torsional strain and/or other steric repulsions in the 13-membered-ring folding patterns, because the amide-to-amide hydrogen bonds should be enthalpically similar for PLL and PLG.

The greater extent of α-helical turn formation for PLG relative to PLL is interesting in light of several studies that have suggested that alanine has a larger α-helix-forming tendency than does glycine. This conclusion has emerged from statistical analysis of protein crystal structures,[26] from conformational stability determinations involving mutant proteins,[27] and from model studies employing synthetic helix-forming peptides.[28] Perhaps most relevant to our results are the studies of Scheraga et al. on helix–coil equilibria in random copolymers made from one of the 20 common amino acids (the "guest" residue) and hydroxypropyl- or hydroxybutyl-L-glutamine (the "host" polymer).[29] Scheraga et al. interpreted the results of these host–guest studies in terms of the theory of Zimm and Bragg,[30] which describes the helix–coil equilibrium in terms of an equilibrium constant, σ, for helix initiation (which may, perhaps too simplistically, be considered to be formation of a single α-helical turn) and an equilibrium constant, *s*, for helix propagation (addition of a residue to an existing helix). The behavior of the host–guest copolymers in aqueous solution was analyzed by Scheraga et al. to generate helix nucleation and propagation parameters for each of the common amino acid residues.[29] The propagation parameters (*s*-values) are generally taken to correspond to the helix-forming tendencies obtained in other studies of model peptides and proteins.[27-28]

Formation of a single α-helical turn in the depsipeptides we have examined is a model for helix initiation, and our results should therefore be compared to σ-values reported by Scheraga et al. These workers found alanine ($\sigma = 8 \times 10^{-4}$) to be a better nucleator than glycine ($\sigma = 1 \times 10^{-5}$).[29] In contrast, our data indicate that the α-helical turn is more highly populated for PLG than for PLL in CH_2Cl_2 at all temperatures examined. These observations suggest that, in some sequence contexts, glycine may

(26) (a) Chou, P. Y.; Fasman, G. D. *Adv. Enzymol.* **1978**, *47*, 45. (b) Barlow, D. J.; Thornton, J. M. *J. Mol. Biol.* **1988**, *201*, 601. (c) Richardson, J. S.; Richardson, D. C. *Science* **1988**, *240*, 1648. (d) MacArthur, M. W.; Thornton, J. M. *J. Mol. Biol.* **1991**, *218*, 397.

(27) See, for example: Horovitz, A.; Matthews, J. M.; Fersht, A. R. *J. Mol. Biol.* **1992**, *227*, 560.

(28) (a) O'Neil, K. T.; DeGrado, W. F. *Science* **1990**, *250*, 646. (b) Strehlow, K. G.; Robertons, A. D.; Baldwin, R. L. *Biochemistry* **1991**, *30*, 5810.

(29) Wojcik, J.; Altmann, K.-H.; Scheraga, H. A. *Biopolymers* **1990**, *30*, 121 and references therein.

(30) Zimm, B. H.; Bragg, J. K. *J. Chem. Phys.* **1959**, *31*, 526.

be superior to alanine for α-helix initiation.[31] The quantitative differences between PLL and PLG suggest that it may be overly simplistic to assume that any residue can be characterized by a single initiation parameter (σ-value). Fersht et al. have made the related point that amino acid residues cannot realistically be assigned "a unique *s*-value that is generally applicable to all positions in all helices in all proteins."[27] These workers determined the effects on conformational stability of alanine vs glycine at various α-helical positions in barnase. The residue swaps had highly variable effects on protein stability, depending upon the position in the α-helix at which the swap occurred. Fersht et al. rationalized these site-dependent differences in terms of variations in the amount of hydrophobic and hydrophilic surface area buried in the folded state. This rationalization requires that the solvation forces play a crucial role in site-dependent differences in helix-forming tendencies. If the conformational properties of α-amino acid residues are adequately reproduced by α-hydroxy acid residues, then our results suggest that glycine can be superior to alanine for α-helical turn formation, even in the absence of strong solvation forces.

α-Helical Turn Formation: PLL vs ALL. Various approaches to estimating the helix-forming tendency of proline agree that this residue is not well suited to α-helical structure.[26-29] Proline's status as an "α-helix breaker" has at least two origins: (i) the lack of an amide proton at the proline residue's nitrogen precludes formation of an intrahelical hydrogen bond and (ii) the bulk of the pyrrolidine ring cannot be easily accommodated in the middle regions of a regular α-helix. Richardson and Richardson, however, have detected a statistically significant tendency for proline residues in crystalline proteins to occur at the so-called N1 position of α-helices, the first N-terminal residue in a fully α-helical conformation.[26c] Causal relationships cannot be unambiguously established by inspection of static structures, but these authors speculated that "in this one location, at least, it seems that Pro is perhaps better described as a helix-initiator than a helix-breaker." Others have suggested that this common occurrence near the N-termini of α-helices indicates proline to be a "helix stop" signal toward residues to the proline's N-terminal side rather than an initiator toward residues to the proline's C-terminal side.[28b] Yun et al. examined this question with constrained molecular dynamics calculations. These workers concluded that proline is, indeed, a helix initiator toward residues to the C-terminal side, because, for simulated polyalanine fragments, proline at the N1 position led to a more favorable free energy for α-helix formation from random coil than did alanine at the N1 position.[32] Strehlow et al. addressed this question experimentally by determining the effect of proline-for-alanine substitutions in a 13-residue peptide with a high intrinsic helix-forming propensity in aqueous solution.[28b] Based on comparison between their observations and predictions derived from the Lifson–Roig theory for helix–coil equilibrium, these workers concluded that proline residues destabilize α-helical conformations in residues to their C-terminal side and do not stabilize α-helical conformations to their N-terminal side. Recently reported studies of other short alanine-rich peptides, however, have indicated that such systems may form 3_{10}-helices instead of α-helices in water,[33] and the conclusions of Strehlow et al. must therefore be treated with caution at present.

Our comparison between PLL and ALL represents an attempt to compare the effects of proline and alanine at the N-terminal position on the stability of a single α-helical turn, i.e., on the thermodynamics of helix initiation. Both NMR and IR data indicate that PLL experiences a greater extent of α-helical turn formation than does ALL in CH_2Cl_2 at all temperatures examined. Further, the observation of relatively small temperature dependences for the C-terminal ΔδNH values of both depsipeptides suggests that the advantage conferred by the proline residue on hydrogen-bonded 13-membered-ring closure is largely entropic. This qualitative thermodynamic conclusion is interesting because we have previously shown that incorporation of rigidifying elements into diamide backbones can either stabilize or destabilize 8- and 9-membered hydrogen-bonded rings and that stabilization resulting from rigidifying elements can be either enthalpic or entropic.[19b]

Our comparison of the folding behavior of PLL and ALL does not address one important question regarding the effect of an N-terminal proline residue on α-helical turn formation along a peptide backbone. In a polypeptide, the proline residue will promote 10-membered-ring hydrogen-bonding (β-turn formation across the Pro-Xxx segment) in addition to promoting α-helical turn formation across the Pro-Xxx-Yyy segment. We have previously reported that PG and PL are nearly completely hydrogen-bonded in the β-turn mode at room temperature in CH_2Cl_2.[10e] No competition is possible between β- and α-helical turns involving the N-terminal carbonyl of PLL, because the depsipeptide backbone does not contain an amide proton at the appropriate position. Analysis of 10- vs 13-membered-ring hydrogen-bond formation in the depsipeptide PLA would allow us to determine whether the proline residue more effectively promotes the β-turn or the α-helical turn.

Conclusions. We have provided the first thermodynamic data for the folding of depsipeptides in solution. These data should prove useful for evaluating the accuracy with which computational methods reproduce the conformational behavior of depsipeptides. (The question of computational accuracy for phenomena controlled by networks of noncovalent interactions has been highlighted by recent reports that some popular computational methods do not correctly predict the hydrogen-bond-mediated folding of simple di- and triamides in organic solvents.[23]) To the extent that the folding properties of our depsipeptides mimic the behavior of analogous peptide backbones, our results suggest that the effect of a given residue on α-helix initiation may depend upon the sequence context of that residue. This implication runs counter to previous proposals that the helix-initiating properties of each residue can be characterized by a single σ-value.[29] Since this study represents the first experimental attempt (as far as we know) to characterize formation of a single α-helical turn in solution, the results should contribute to the deconvolution of local and nonlocal forces that will ultimately be required for a thorough understanding of protein folding preferences.

Experimental Section

General. Melting points are uncorrected. THF was distilled from Na/K/benzophenone under N_2, and CH_2Cl_2 was distilled from CaH_2 under N_2. Other solvents and reagents were reagent grade and used as obtained, except for hexane (for chromatography), which was flash distilled. The synthesis and characterization of acetyl-L-lactate-*N*-methylamide (L) have been previously described;[34] the preparation of other depsipeptides is given below. Thin-layer chromatography was carried out with silica gel 60 F-524 plates from EM Science. Column chromatography was carried out using low N_2 pressure with 230–400-mesh silica gel (EM Science). When columns were eluted with MeOH in $CHCl_3$, they were slurry-packed after the silica gel had been stirred with the eluant for several hours. Fresh solvent was then passed through the column continuously until subtle changes in the gray hue of the silica had moved completely through the column bed. This preequilibration was essential for optimal resolution.

Routine characterization ^1H NMR spectroscopy was performed on a Bruker WP-200 spectrometer. ^{13}C NMR spectra were obtained on either

(31) The preference for G over L at the third residue of the PLX depsipeptides is not related to the common occurrence of glycine residues at the so-called C-cap position of α-helices in crystalline proteins (ref 26c), which involves a non-α-helical conformation for the glycine in question and a hydrogen-bonding pattern different from that of the 13-membered ring. This hydrogen-bonding pattern would be impossible in PLG.

(32) Yun, R. H.; Anderson, A.; Hermans, J. *Proteins: Struct., Funct. Gent.* **1991**, *10*, 219.

(33) Miick, S. M.; Martinez, G. V.; Fiori, W. R.; Todd, A. P.; Millhauser, G. L. *Nature* **1992**, *359*. 653.

(34) Ingwall, R. T.; Gilon, C.; Goodman, M. *Macromolecules* **1976**, *9*, 802.

a Bruker WP-270 or an AM-500 spectrometer. Chemical shifts are reported relative to tetramethylsilane (0 ppm) or relative to the isotopic impurity peak for a given solvent ($CDCl_3$, 7.26 ppm for ^1H and 77.0 ppm for ^{13}C; CD_3CN, 1.93 ppm for ^1H and 1.3 ppm for ^{13}C; CD_2Cl_2, 5.32 ppm for ^1H; DMSO-d_6, 2.49 ppm for ^1H). IR measurements were performed on a Nicolet 740 spectrometer equipped with a TGS detector. High-resolution electron impact mass spectroscopy was performed on a Kratos MS-25 spectrometer. Variable-temperature IR and ^1H NMR spectroscopic experiments were performed as previously described.[20] The purity of compounds used for variable-temperature spectroscopic experiments was judged to be >95% by high-field ^1H NMR spectroscopy. Curve-fitting analysis of IR spectra was carried out with the FOCAS v2.2 program from Nicolet.[35]

Ac-Glyco-NHMe (G). Glycolic acid (2.0 g, 26 mmol) was allowed to react with *N*-hydroxysuccinimide (4.5 g, 39 mmol) and dicyclohexylcarbodiimide (6.8 g, 33 mmol) in THF (80 mL) at 0 °C for 3 h. Anhydrous methylamine was bubbled for 10 min through the white slurry, and stirring was continued for 5 h as the reaction mixture warmed to room temperature. The slurry was suction-filtered, and the filtrate was concentrated and purified by chromatography (5 vol % MeOH in $CHCl_3$) to yield the *N*-methylamide of glycolic acid as a white solid (1.8 g, 76%): mp 63–65 °C; R_f 0.24 (10 vol % MeOH in $CHCl_3$); ^1H NMR (200 MHz, $CDCl_3$) δ 6.94 (broad, 1 H), 4.52 (broad, 1 H), 4.05 (s, 2 H), 2.86 (d, J = 4.9 Hz, 3 H); ^{13}C NMR (67.5 MHz, $CDCl_3$) δ 173.49 (C), 61.81 (CH_2), 25.51 (CH_3); EI MS m/e 89.0473, calcd for $C_3H_7NO_2$ 89.0477.

A solution of this amide (0.31 g, 3.4 mmol) and 4-(dimethylamino)pyridine (0.04 g, 0.3 mmol) in CH_2Cl_2 (10 mL) was cooled to 0 °C and treated with acetyl chloride (0.48 mL, 6.8 mmol). The reaction mixture was allowed to warm to room temperature over 12 h. The slurry was suction-filtered, and volatiles were removed at a rotary evaporator. The resulting residue was purified by chromatography (5 vol % MeOH in $CHCl_3$) to provide G as a white solid (0.30 g, 67%): mp 41.0–41.5 °C; R_f 0.65 (15 vol % MeOH in $CHCl_3$); ^1H NMR (270 MHz, $CDCl_3$) δ 6.92 (broad, 1 H), 4.57 (s, 2 H), 2.85 (d, J = 5.0 Hz, 3 H), 2.17 (s, 3 H); ^{13}C NMR (125 MHz, $CDCl_3$) δ 169.32 (C), 167.50 (C), 62.97 (CH_2), 25.80 (CH_3), 20.68 (CH_3); IR (1 mM in CH_2Cl_2) 3454, 1756, 1685, 1541 cm^{-1}; EI MS, m/e 131.0582, calcd for $C_5H_9NO_3$ 131.0582.

Ac-L-Ala-OMe (A-OMe). A solution of L-alanine methyl ester hydrochloride (0.20 g, 1.5 mmol) and triethylamine (0.50 mL, 3.6 mmol) in DMF (5 mL) was cooled to 0 °C and treated with acetyl chloride (0.20 mL, 2.2 mmol). The reaction mixture was allowed to warm to room temperature over 5 h. The slurry was suction-filtered, and volatiles were removed at a vacuum rotary evaporator. The resulting residue was purified by chromatography (70–100 vol % EtOAc in hexanes) to provide A-OMe as a colorless oil (0.10 g, 47%): R_f 0.33 (EtOAc); ^1H NMR (270 MHz, $CDCl_3$) δ 6.11 (broad, 1 H), 4.60 (quintet, J = 7.3 Hz, 1 H), 3.75 (s, 3 H), 2.02 (s, 3 H), 1.40 (d, J = 7.3 Hz, 3 H); ^{13}C NMR (125 MHz, $CDCl_3$) δ 173.54 (C), 169.76 (C), 52.27 (CH), 47.86 (CH_3), 22.84 (CH_3), 18.12 (CH_3); IR (1 mM in CH_2Cl_2) 3432, 1742, 1679, 1512 cm^{-1}; EI MS m/e 145.0746, calcd for $C_6H_{11}NO_3$ 145.0739.

Ac-L-Lac-L-Lac-NHMe (LL). To a solution of L-lactic acid (5.4 g, 60.0 mmol) and 1,8-diazabicyclo[5.4.0]undec-7-ene (9.0 mL, 60.0 mmol) in benzene (400 mL) was added benzyl bromide (8.6 mL, 72.0 mmol) in benzene (50 mL) via cannula.[36] After being refluxed for 5 h, the reaction mixture was cooled to room temperature, diluted with Et_2O (300 mL), and suction-filtered. This solid was washed with Et_2O, and the combined organic filtrates were washed successively with H_2O (200 mL), 0.5 M HCl (200 mL), dilute $NaHCO_3$ (200 mL), and H_2O (200 mL). The resulting organic layer was dried over Na_2SO_4 and concentrated. Chromatography (20 vol % EtOAc in hexanes) yielded benzyl L-lactate as a colorless liquid (9.5 g, 88%): R_f 0.43 (50 vol % EtOAc in hexanes); ^1H NMR (200 MHz, $CDCl_3$) δ 7.35 (s, 5 H), 5.19 (s, 2 H), 4.34–4.28 (m, 1 H), 3.04 (d, J = 5.4 Hz, 1 H), 1.42 (d, J = 6.9 Hz, 3 H); ^{13}C NMR (125 MHz, $CDCl_3$) δ 175.37 (C), 135.13 (C), 128.51 (CH), 128.38 (CH), 128.09 (CH), 67.12 (CH2), 66.74 (CH), 20.26 (CH_3); EI MS m/e 180.0789, calcd for $C_{10}H_{12}O_3$ 180.0786. This material was carried on immediately to the next step.

A solution of benzyl L-lactate (1.3 g, 7.0 mmol) and triethylamine (1.5 mL, 10.0 mmol) in CH_2Cl_2 (25 mL) was cooled to 0 °C and treated with acetyl chloride (0.75 mL, 10.0 mmol). The reaction mixture was allowed to warm to room temperature over 5 h. The slurry was suction-filtered, and volatiles were removed at a rotary evaporator. The residue was purified by chromatography (10 vol % EtOAc in hexanes) to yield a colorless liquid (0.78 g, 50% crude): R_f 0.25 (10 vol % EtOAc in hexanes); ^1H NMR (200 MHz, $CDCl_3$) δ 7.33 (s, 5 H), 5.15 (s, 2 H), 5.10 (q, 7.1 Hz, 1 H), 2.13 (s, 3 H), 1.49 (d, J = 7.1 Hz, 3 H). A solution of this material in EtOAc (7 mL) and 5% Pd–C (0.23 g) were placed in a round-bottom flask fitted with a hydrogen-filled balloon and water aspirator connection. The system was flushed three times with hydrogen, and the suspension was stirred for 5 h under positive hydrogen pressure. The catalyst was removed by gravity filtration using qualitative grade filter paper, and the filtrate was concentrated. Acetyl-L-lactic acid was isolated as a colorless viscous liquid (0.44 g, 48%): ^1H NMR (200 MHz, $CDCl_3$) δ 9.76 (broad, 1 H), 5.09 (q, J = 7.1 Hz, 1 H), 2.14 (s, 3 H), 1.53 (d, J = 7.1 Hz, 3 H); ^{13}C NMR (125 MHz, $CDCl_3$) δ 176.58 (C), 170.47 (C), 68.19 (CH), 20.59 (CH_3), 16.79 (CH_3); EI MS m/e 131.0341, calcd for $C_5H_8O_4$ – H: 131.0344. This material was carried on immediately to the next step.

A solution of acetyl-L-lactic acid (0.35 g, 2.6 mmol), the *N*-methylamide of L-lactic acid (0.27 g, 2.6 mmol), and 4-(dimethylamino)pyridine (0.03 g, 0.3 mmol) in CH_2Cl_2 (8 mL) was cooled to 0 °C, treated with dicyclohexylcarbodiimide (0.68 g, 3.3 mmol), and allowed to warm to room temperature over 5 h. The slurry was suction-filtered, and the filtrate was concentrated. Chromatography (70–100% vol % EtOAc in hexanes) provided LL as a viscous liquid (0.55 g, 97%): R_f 0.44 (EtOAc); ^1H NMR (500 MHz, $CDCl_3$) δ 6.26 (broad, 1 H), 5.25 (q, J = 6.9 Hz, 1 H), 5.05 (q, J = 7.1 Hz, 1 H), 2.82 (d, J = 4.8 Hz, 3 H), 2.17 (s, 3 H), 1.55 (d, J = 7.1 Hz, 3 H), 1.50 (d, J = 6.9 Hz, 3 H); ^{13}C NMR (125 MHz, $CDCl_3$) δ 171.64 (C), 170.41 (C), 169.37 (C), 71.53 (CH), 69.17 (CH), 26.06 (CH_3), 20.75 (CH_3), 17.67 (CH_3), 16.77 (CH_3); IR (1 mM in CH_2Cl_2) 3458, 3416, 1763, 1746, 1681, 1539 cm^{-1}; EI MS m/e 217.0963, calcd for $C_9H_{15}NO_5$ 217.0950.

Ac-L-Lac-Glyco-NHMe (LG). A solution of acetyl-L-lactic acid (0.22 g, 1.7 mmol), the *N*-methylamide of glycolic acid (0.15 g, 1.7 mmol), and 4-(dimethylamino)pyridine (0.02 g, 0.2 mmol) in CH_2Cl_2 (5 mL) was cooled to 0 °C, treated with dicyclohexylcarbodiimide (0.44 g, 2.1 mmol), and allowed to warm to room temperature over 4 h. The slurry was suction-filtered, and the filtrate was concentrated. Chromatography (EtOAc) provided LG as a white powdery solid (0.19 g, 57%): mp 96.5–97.5 °C; R_f 0.25 (EtOAc); ^1H NMR (200 MHz, $CDCl_3$) δ 6.52 (broad, 1 H), 4.98 (q, J = 7.1 Hz, 1 H), 4.76 (AB q, A part, J = 15.3 Hz, 1 H), 4.57 (AB q, B part, J = 15.3 Hz, 1 H), 2.86 (d, J = 4.8 Hz, 3 H), 2.17 (s, 3 H), 1.54 (d, J = 7.1 Hz, 3 H); ^{13}C NMR (125 MHz, $CDCl_3$) δ 171.53 (C), 169.90 (C), 167.14 (C), 69.28 (CH), 63.08 (CH_2), 25.89 (CH_3), 20.57 (CH_3), 16.53 (CH_3); IR (1 mM in CH_2Cl_2) 3452, 3419, 1766, 1743, 1684, 1558, 1544 cm^{-1}; EI MS m/e 203.0791, calcd for $C_8H_{13}NO_5$ 203.0794.

Ac-Glyco-L-Lac-NHMe (GL). The benzyl ester of glycolic acid was synthesized according to the procedure described for benzyl L-lactate: glycolic acid (4.0 g, 53 mmol), 1,8-diazabicyclo[5.4.0]undec-7-ene (8.0 mL, 53 mmol), and benzyl bromide (7.5 mL, 63 mmol) in benzene (350 mL) were refluxed for 2.5 h. Workup and chromatography (10–50 vol % EtOAc in hexanes) yielded a colorless liquid (7.4 g, 84%): R_f 0.40 (50 vol % EtOAc in hexanes); ^1H NMR (200 MHz, $CDCl_3$) δ 7.36 (s, 5 H), 5.21 (s, 2 H), 4.19 (s, 2 H), 2.69 (broad, 1 H); EI MS m/e 166.0636, calcd for $C_9H_{10}O_3$ 166.0630. This material was carried on immediately to the next step.

A solution of benzyl glycolate (1.5 g, 8.8 mmol) and triethylamine (1.8 mL, 13 mmol) in CH_2Cl_2 (25 mL) was cooled to 0 °C and treated with acetyl chloride (0.94 mL, 13 mmol). The reaction mixture was allowed to warm to room temperature over 4 h. The slurry was suction-filtered, and volatiles were removed at a rotary evaporator. The residue was purified by chromatography (25 vol % EtOAc in hexanes) to yield a colorless liquid: R_f 0.65 (50 vol % EtOAc in hexanes). This material was taken up in absolute EtOH (20 mL) and hydrogenated with 5% Pd–C (0.62 g) for 5 h. Acetyl glycolic acid was isolated as a colorless viscous liquid (0.88 g, 85%): ^1H NMR (200 MHz, $CDCl_3$) δ 11.4 (broad, 1 H), 4.67 (s, 2 H), 2.15 (s, 3 H); EI MS m/e 118.0272, calcd for $C_4H_6O_4$ 118.0266. This material was carried on immediately to the next step.

A solution of acetyl glycolic acid (0.25 g, 2.1 mmol), the *N*-methylamide of L-lactic acid (0.22 g, 2.2 mmol), and 4-(dimethylamino)pyridine (0.03 g, 0.2 mmol) in CH_2Cl_2 (8 mL) was cooled to 0 °C, treated with dicyclohexylcarbodiimide (0.46 g, 2.2 mmol), and allowed to warm to room temperature over 4 h. The slurry was suction-filtered, and the filtrate was concentrated. Chromatography (EtOAc) provided LG as a colorless oil (0.21 g, 49%): R_f 0.57 (10 vol % MeOH in $CHCl_3$); ^1H NMR (270 MHz, $CDCl_3$) δ 6.60 (broad, 1 H), 5.28 (q, J = 7.0 Hz, 1 H), 4.66 (s, 2 H), 2.82 (d, J = 4.8 Hz, 3 H), 2.18 (s, 3 H), 1.50 (d, J

(35) For details on the curve-fitting protocol, see: Gallo, E. A.; Ph.D. Thesis, University of Wisconsin—Madison, 1992.

(36) Ono, N.; Yamada, T.; Saito, T.; Tanaka, K.; Kaji, A. *Bull. Chem. Soc. Jpn.* **1978**, *51*, 2401.

= 7.0, 3 H); ^{13}C NMR (125 MHz, $CDCl_3$) δ 171.07 (C), 170.18 (C), 166.57 (C), 71.50 (CH), 61.14 (CH_2), 26.07 (CH_3), 20.42 (CH_3), 17.68 (CH_3); IR (1 mM in CH_2Cl_2) 3459, 3425, 1767, 1752, 1682, 1541 cm^{-1}; EI MS *m/e* 203.0798, calcd for $C_8H_{13}NO_5$ 203.0794.

Ac-Glyco-Glyco-NHMe (GG). A solution of acetyl glycolic acid (0.25 g, 2.1 mmol), the *N*-methylamide of glycolic acid (0.19 g, 2.2 mmol), and 4-(dimethylamino)pyridine (0.03 g, 0.2 mmol) in CH_2Cl_2 (8 mL) was cooled to 0 °C, treated with dicyclohexylcarbodiimide (0.46 g, 2.2 mmol), and allowed to warm to room temperature over 4 h. The slurry was suction-filtered, and the filtrate was concentrated. Chromatography (EtOAc) provided GG as a colorless oil (0.28 g, 70%): R_f 0.52 (10 vol % MeOH in $CHCl_3$); ^{1}H NMR (270 MHz, $CDCl_3$) δ 6.41 (broad, 1 H), 4.67 (s, 2 H), 4.66 (s, 2 H), 2.86 (d, *J* = 4.8 Hz, 3 H), 2.19 (s, 3 H); ^{13}C NMR (125 MHz, $CDCl_3$) δ 171.02 (C), 166.98 (C), 166.65 (C), 63.10 (CH_2), 60.90 (CH_2), 25.86 (CH_3), 20.35 (CH_3); IR (1 mM in CH_2Cl_2) 3453, 3421, 1772, 1754, 1685, 1548 cm^{-1}; EI MS *m/e* 189.0628, calcd for $C_7H_{11}NO_5$ 189.0637.

Ac-L-Pro-L-Lac-L-Lac-NHME (PLL). A solution of *N*-acetyl-L-proline (1.8 g, 12 mmol), benzyl L-lactate (2.1 g, 12 mmol), and 4-(dimethylamino)pyridine (0.14 g, 1.2 mmol) in CH_2Cl_2 (30 mL) was cooled to 0 °C, treated with dicyclohexylcarbodiimide (3.0 g, 15 mmol), and allowed to warm to room temperature over 3 h. The slurry was suction-filtered, and the filtrate was concentrated. Purification by chromatography (70 vol % EtOAc in hexanes) provided a colorless oil: R_f 0.32 (EtOAc). This material was taken up in absolute EtOAc (15 mL) and hydrogenated with 5% Pd–C (0.55 g) for 18 h. Ac-L-Pro-L-Lac-OH was isolated as a white solid (2.5 g, 93% crude): ^{1}H NMR (200 MHz, $CDCl_3$) δ 9.12 (broad, 1 H), 5.16 (q, *J* = 7.1 Hz, 1 H), 4.61–4.55 (m, 1 H), 3.73–3.44 (m, 2 H), 2.45–1.85 (m, 4 H), 2.13 (s, 3 H), 1.54 (d, *J* = 7.1 Hz, 3 H), and ca. 20% minor rotamer, δ 4.47–4.43 (m); EI MS *m/e* 229.0937, calcd for $C_{10}H_{15}NO_5$ 229.0950. This material was carried on immediately to the next step.

A solution of crude Ac-L-Pro-L-Lac-OH (0.70 g, 3.0 mmol), the *N*-methylamide of L-lactic acid (0.32 g, 3.1 mmol), and 4-(dimethylamino)pyridine (0.04 g, 0.3 mmol) in CH_2Cl_2 (10 mL) was cooled to 0 °C, treated with dicyclohexylcarbodiimide (0.78 g, 3.8 mmol), and allowed to warm to room temperature over 4 h. The slurry was suction-filtered, and the filtrate was concentrated. Chromatography (4 vol % MeOH in $CHCl_3$) provided PLL as a white powdery solid (0.55 g, 58%): mp 90–91 °C; R_f 0.37 (5 vol % MeOH in $CHCl_3$); ^{1}H NMR (270 MHz, $CDCl_3$) δ 6.72 (broad, 1 H), 5.25 (q, *J* = 6.9 Hz, 1 H), 5.14 (q, *J* = 7.1 Hz, 1 H), 4.58–4.52 (m, 1 H), 3.75–3.50 (m, 2 H), 2.82 (d, *J* = 4.5 Hz, 3 H), 2.40–2.00 (m, 4 H), 2.11 (s, 3 H), 1.56 (d, *J* = 7.1 Hz, 3 H), 1.48 (d, *J* = 6.9 Hz, 3 H), and ca. 10% minor rotamer, δ 6.13 (broad), 5.24 (q), 5.15 (q), 1.61 (d), 1.50 (d); ^{13}C NMR (67.5 MHz, $CDCl_3$) δ 172.07 (C), 170.26 (C), 169.37 (C), 169.02 (C), 71.40 (CH), 69.14 (CH), 58.26 (CH), 47.57 (CH_2), 28.99 (CH_2), 25.75 (CH_3), 24.57 (CH_2), 21.97 (CH_3), 17.70 (CH_3), 16.54 (CH_3) and minor rotamer, δ 69.2, 59.5, 47.0; IR (1 mM in CH_2Cl_2) 3454, 3409, 3365, 1746, 1678, 1647, 1545 cm^{-1}; EI MS *m/e* 314.1472, calcd for $C_{14}H_{22}N_2O_6$ 314.1478.

Ac-L-Ala-L-Lac-L-Lac-NHMe (ALL). A solution of *N*-(*tert*-butoxycarbonyl)-L-alanine (2.4 g, 13 mmol), benzyl L-lactate (2.3 g, 13 mmol), and 4-(dimethylamino)pyridine (1.6 g, 13 mmol) in CH_2Cl_2 (250 mL) was cooled to 0 °C, treated with dicyclohexylcarbodiimide (3.0 g, 14 mmol), and allowed to warm to room temperature overnight. The reaction mixture was suction-filtered, and the filtrate was washed with 5 wt % $NaHSO_4$. The organic layer was concentrated and allowed to stand for 2 days, resulting in the precipitation of an oily crystalline material (4.5 g). This material (1.6 g) was taken up in absolute EtOH (18 mL) and hydrogenated with 5% Pd–C (0.38 g) for 15 h. The resulting oil was partitioned between EtOAc and dilute aqueous $NaHCO_3$. The aqueous layer was cooled to 0 °C, acidified carefully with 1 M HCl to pH 3, and washed with EtOAc. The organic layer was dried over $MgSO_4$ and concentrated, and tBoc-L-Ala-L-Lac-OH was isolated as a colorless oil (0.82 g, 60%): ^{1}H NMR (200 MHz, DMSO-d_6) δ 7.30 (d, *J* = 7.2 Hz, 1 H), 4.93 (q, *J* = 7.2 Hz, 1 H), 4.20–3.80 (m, 1 H), 1.40 (d, *J* = 7.2 Hz, 3 H), 1.38 (s, 9 H), 1.28 (d, *J* = 7.2 Hz, 3 H), CO_2H not observed. This material was carried on immediately to the next step.

A solution of crude tBoc-L-Ala-L-Lac-OH (0.75 g, 2.9 mmol), the *N*-methylamide of L-lactic acid (0.32 g, 3.1 mmol), and 4-(dimethylamino)pyridine (0.04 g, 0.3 mmol) in CH_2Cl_2 (10 mL) was cooled to 0 °C, treated with dicyclohexylcarbodiimide (0.74 g, 3.6 mmol), and allowed to warm to room temperature over 5 h. The slurry was suction-filtered, and the filtrate was concentrated. Chromatography (50–70 vol % EtOAc in hexanes) provided an off-white solid (0.76 g, 77%): ^{1}H NMR (200 MHz, $CDCl_3$) δ 6.51 (broad, 1 H), 5.25 (q, *J* = 6.8 Hz, 1 H), 5.11 (q, *J* = 7.1 Hz, 1 H), 5.08 (broad d, *J* = 7.1 Hz, 1 H), 4.35 (quintet, *J* = 7.1 Hz, 1 H), 2.83 (d, *J* = 4.8 Hz, 3 H), 1.58 (d, *J* = 7.1 Hz, 3 H), 1.47 (d, *J* = 7.1 Hz, 3 H), 1.45 (s, 9 H), 1.44 (d, *J* = 6.8 Hz, 3 H). This material was carried on immediately to the next step.

The crude solid from the previous reaction (0.73 g, 2.1 mmol) was stirred in 4 N HCl in dioxane (5 mL, 20 mmol) for 1 h. Volatiles were removed at a vacuum rotary evaporator, and the resulting foamy off-white material was dried in vacuo for several hours. DMF (15 mL) was added, and the solution was cooled to 0 °C. Triethylamine (0.75 mL, 5.4 mmol) and acetyl chloride (0.22 mL, 3.1 mmol) were added, and stirring was continued at 0 °C for 5 h. The resulting slurry was suction-filtered, and volatiles were removed at a vacuum rotary evaporator. The residue was purified by chromatography (3–4 vol % MeOH in $CHCl_3$). ALL was isolated as a white solid 57 (0.45 g, 74%): mp 114–115 °C; R_f 0.14 (3 vol % MeOH in $CHCl_3$); ^{1}H NMR (270 MHz, $CDCl_3$) δ 6.64 (broad, 1 H), 6.54 (d, *J* = 7.1 Hz, 1 H), 5.22 (q, *J* = 6.8 Hz, 1 H), 5.13 (q, *J* = 7.1 Hz, 1 H), 4.56 (quintet, *J* = 7.1 Hz, 1 H), 2.83 (d, *J* = 4.8 Hz, 3 H), 2.04 (s, 3 H), 1.57 (d, *J* = 7.1 Hz, 3 H), 1.48 (d, *J* = 6.8 Hz, 3 H), 1.47 (d, *J* = 7.1 Hz, 3 H); ^{13}C NMR (67.5 MHz, $CDCl_3$) δ 173.08 (C), 170.38 (C), 170.15 (C), 168.98 (C), 71.49 (CH), 69.40 (CH), 48.13 (CH), 25.96 (CH_3), 22.64 (CH_3), 17.65 (CH_3), 17.39 (CH_3), 16.58 (CH_3); IR (1 mM in CH_2Cl_2) 3440, 1746, 1680, 1541, 1510 cm^{-1}; EI MS *m/e* 288.1330, calcd for $C_{12}H_{20}N_2O_6$ 288.1321.

Ac-L-Pro-L-Lac-Glyco-NHMe (PLG). A solution of crude Ac-L-Pro-L-Lac-OH (0.39 g, 1.7 mmol), the *N*-methylamide of glycolic acid (0.16 g, 1.7 mmol), and 4-(dimethylamino)pyridine (0.02 g, 0.2 mmol) in CH_2Cl_2 (5 mL) was cooled to 0 °C, treated with dicyclohexylcarbodiimide (0.44 g, 2.1 mmol), and allowed to warm to room temperature over 4 h. The slurry was suction-filtered, and the filtrate was concentrated. Chromatography (5 vol % MeOH in $CHCl_3$) provided PLG as a white powdery solid (0.32 g, 62%): mp 89.5–90.0 °C; R_f 0.38 (10 vol % MeOH in $CHCl_3$); ^{1}H NMR (200 MHz, $CDCl_3$) δ 7.00 (broad, 1 H), 5.10 (q, *J* = 7.0 Hz, 1 H), 4.58–4.52 (m, 1 H), 3.70–3.51 (m, 2 H), 2.86 (d, *J* = 4.8 Hz, 3 H), 2.40–2.00 (m, 4 H), 2.11 (s, 3 H), 1.56 (d, *J* = 7.0 Hz, 3 H), and ca. 10% minor rotamer, δ 6.5 (broad); ^{13}C NMR (125 MHz, $CDCl_3$) δ 172.30 (C), 169.68 (C), 169.57 (C), 167.01 (C), 69.45 (CH), 63.48 (CH_2), 58.36 (CH), 47.79 (CH_2), 29.24 (CH_2), 25.93 (CH_3), 24.81 (CH_2), 22.16 (CH_3), 16.64 (CH_3); IR (1 mM in CH_2Cl_2) 3449, 3418, 3359, 1749, 1681, 1647, 1548 cm^{-1}; EI MS *m/e* 300.1320, calcd for $C_{13}H_{20}N_2O_6$ 300.1321.

Ac-L-Pro-Glyco-L-Lac-NHMe (PGL). A solution of *N*-acetyl-L-proline (1.2 g, 7.3 mmol), benzyl glycolate (1.2 g, 7.3 mmol), and 4-(dimethylamino)pyridine (0.09 g, 0.7 mmol) in CH_2Cl_2 (25 mL) was cooled to 0 °C, treated with dicyclohexylcarbodiimide (1.9 g, 9.1 mmol), and allowed to warm to room temperature over 4 h. The slurry was suction-filtered, and the filtrate was concentrated. Purification by chromatography (EtOAc) provided a colorless liquid: R_f 0.44 (50 vol % EtOAc in hexanes). This material was taken up in absolute EtOH (20 mL) and hydrogenated with 5% Pd–C (0.35 g) for 4 h. White solid Ac-L-Pro-Glyco-OH (0.67 g, 87% crude) was isolated: ^{1}H NMR (200 MHz, $CDCl_3$) δ 4.69 (m, 2 H), 4.60–4.54 (m, 1 H), 3.75–3.45 (m, 2 H), 2.40–1.90 (m, 4 H), 2.14 (s, 3 H), $-CO_2H$ not observed; EI MS *m/e* 215.0792, calcd for $C_9H_{13}NO$ 215.0794. This material was carried on immediately to the next step.

A solution of crude Ac-L-Pro-GLyco-OH (0.38 g, 1.8 mmol), the *N*-methylamide of L-lactic acid (0.19 g, 1.8 mmol) and 4-(dimethylamino)pyridine (0.02 g, 0.2 mmol) in CH_2Cl_2 (7 mL) was cooled to 0 °C, treated with dicyclohexylcarbodiimide (0.46 g, 2.2 mmol), and allowed to warm to room temperature over 4 h. The slurry was suction-filtered, and the filtrate was concentrated. Chromatography (5 vol % MeOH in $CHCl_3$) provided PGL as a colorless oil (0.18 g, 33%): R_f 0.29 (10 vol % MeOH in $CHCl_3$); ^{1}H NMR (270 MHz, $CDCl_3$) δ 7.10 (broad, 1 H), 5.28 (q, *J* = 6.8 Hz, 1 H), 4.74 (AB q, A part, *J* = 15.8 Hz, 1 H), 4.67 (AB q, B part, *J* = 15.8 Hz, 1 H), 4.58–4.52 (m, 1 H), 3.71–3.52 (m, 2 H), 2.83 (d, *J* = 4.7 Hz, 3 H), 2.54–2.00 (m, 4 H), 2.11 (s, 3 H), 1.48 (d, *J* = 6.8 Hz, 3 H), and ca. 10% minor rotamer, δ 6.6 (broad); ^{13}C NMR (125 MHz, $CDCl_3$) δ 172.19 (C), 170.32 (C), 169.57 (C), 166.23 (C), 72.01 (CH), 61.29 (CH_2), 58.40 (CH), 47.79 (CH_2), 29.33 (CH_2), 26.06 (CH_3), 24.87 (CH_2), 22.16 (CH_3), 18.01 (CH_3), and minor rotamer, δ 71.9, 60.8, 46.3, 22.7, 17.5; IR (1 mM in CH_2Cl_2) 3459, 3411, 3362, 1753, 1679, 1647, 1544 cm^{-1}; EI MS *m/e* 300.1334, calcd for $C_{13}H_{20}N_2O_6$ 300.1321.

Ac-L-Pro-Glyco-Glyco-NHMe (PGG). A solution of crude Ac-L-Pro-Glyco-OH (0.36 g, 1.7 mmol), *N*-methylamide of glycolic acid (0.15 g, 1.7 mmol), and 4-(dimethylamino)pyridine (0.02 g, 0.2 mmol) in CH_2Cl_2 (7 mL) was cooled to 0 °C, treated with dicyclohexylcarbodiimide (0.44 g, 2.1 mmol), and allowed to warm to room temperature over 4 h. The

slurry was suction-filtered, and the filtrate was concentrated. Chromatography (5 vol % MeOH in $CHCl_3$) provided PGG as a colorless oil (0.29 g, 60%): R_f 0.39 (10 vol % MeOH in $CHCl_3$); ^1H NMR (200 MHz, $CDCl_3$) δ 7.34 (broad, 1 H), 4.79 (AB q, A part, J = 15.9 Hz, 1 H), 4.76 (AB q, B part, J = 15.9 Hz, 1 H), 4.63 (AB q, A part, J = 15.8 Hz, 1 H), 4.57 (AB q, B part, J = 15.8 Hz, 1 H), 4.57–4.51 (m, 1 H), 3.76–3.62 (m, 2 H), 2.84 (d, J = 3.7 Hz, 3 H), 2.35–1.90 (m, 4 H), 2.11 (s, 3 H), and ca. 10% minor rotamer, δ 6.8 (broad); ^{13}C NMR (125 MHz, $CDCl_3$) δ 171.84 (C), 169.43 (C), 166.65 (C), 166.35 (C), 63.45 (CH_2), 60.87 (CH_2), 58.25 (CH), 47.64 (CH_2), 29.17 (CH_2), 25.73 (CH_3), 24.70 (CH_2), 21.94 (CH_3), and minor rotamer, δ 63.1, 60.6, 58.0, 46.1, 29.0, 24.5, 22.4; IR (1 mM in CH_2Cl_2) 3453, 3387, 1757, 1680, 1646, 1549 cm^{-1}; EI MS m/e 286.1158, calcd for $C_{12}H_{18}N_2O_6$ 286.1165.

Ac-L-Ala-Glyco-NMe$_2$ (AG-NMe$_2$). Glycolic acid (1.0 g, 13 mmol) was allowed to react with N-hydroxysuccinimide (2.3 g, 20 mmol) and dicyclohexylcarbodiimide (3.4 g, 16 mmol) in THF (40 mL) at 0 °C for 1 h. Anhydrous dimethylamine was bubbled for 10 min through the white slurry, and stirring was continued for 4 h as the reaction mixture was warmed to room temperature. The slurry was suction-filtered, and the filtrate was concentrated and purified by chromatography (80 vol % EtOAc in hexanes) to yield the N,N-dimethylamide of glycolic acid as a white solid (0.23 g, 17%): R_f 0.18 (EtOAc); ^1H NMR (200 MHz, $CDCl_3$) δ 4.15 (d, J = 4.3 Hz, 2 H), 3.63 (t, J = 4.3 Hz, 1 H), 3.04 (s, 3 H), 2.89 (s, 3 H); EI MS m/e 103.0630, calcd for $C_4H_9NO_2$, 103.0633. This material was carried on immediately to the next step.

A solution of N-(*tert*-butoxycarbonyl)-L-alanine (0.28 g, 1.5 mmol), the N,N-dimethylamide of glycolic acid (0.15 g, 1.5 mmol), and 4-(dimethylamino)pyridine (0.02 g, 0.2 mmol) in CH_2Cl_2 (5 mL) was cooled to 0 °C, treated with dicyclohexylcarbodiimide (0.39 g, 1.9 mmol), and allowed to warm to room temperature over 5 h. The slurry was suction-filtered, and the filtrate was concentrated. Chromatography (70–100% vol % EtOAc in hexanes) provided a white crystalline solid (0.31 g, 76%): R_f 0.24 (70 vol % EtOAc in hexanes); ^1H NMR (200 MHz, $CDCl_3$) δ 5.06 (d, J = 7.2 Hz, 1 H), 4.88 (AB q, A part, J = 14.4 Hz, 1 H), 4.68 (AB q, B part, J = 14.4 Hz, 1 H), 4.43 (quintet, J = 7.2 Hz, 1 H), 2.98 (s, 3 H), 2.97 (s, 3 H), 1.50 (d, J = 7.2 Hz, 3 H), 1.44 (s, 9 H); EI MS m/e 275.1600, calcd for $C_{12}H_{22}H_2O_5$ + H, 275.1607. This material was carried on immediately to the next step.

Crude tBoc-L-Ala-Glyco-NMe$_2$ (0.29 g, 1.1 mmol) was stirred in 4 N HCl in dioxane (5 mL, 20 mmol) for 3 h. Volatiles were removed at a vacuum rotary evaporator, and the resulting foamy off-white material was dried in vacuo overnight DMF (10 mL) was added, and the solution was cooled to 0 °C. Triethylamine (0.37 mL, 2.7 mmol) and acetyl chloride (0.11 mL, 1.6 mmol) were added, and stirring was continued at 0 °C for 5 h. The resulting slurry was suction-filtered, and volatiles were removed at a vacuum rotary evaporator. The residue was purified by chromatography (3–5 vol % MeOH in $CHCl_3$), and AG-NMe$_2$ was obtained as a white crystalline solid (0.19 g, 82%): mp 79.5–80.5 °C; R_f 0.19 (5 vol % MeOH in $CHCl_3$); ^1H NMR (200 MHz, $CDCl_3$) δ 6.30 (d, J = 7.2 Hz, 1 H), 4.87 (AB q, A part, J = 14.4 Hz, 1 H), 4.70 (AB q, B part, J = 14.4 Hz, 1 H), 4.70 (quintet, J = 7.2 Hz, 1 H), 2.98 (s, 3 H), 2.97 (s, 3 H), 2.02 (s, 3 H), 1.51 (d, J = 7.2 Hz, 3 H); ^{13}C NMR (67.5 MHz, $CDCl_3$) δ 172.77 (C), 169.65 (C), 165.73 (C), 61.67 (CH_2), 48.08 (CH), 35.67 (CH_3), 35.51 (CH_3), 23.03 (CH_3), 18.24 (CH_3); IR (1 mM in CH_2Cl_2) 3443, 1749, 1719, 1672, 1510 cm^{-1}; EI MS m/e 216.1093, cacld for $C_9H_{16}N_2O_4$, 216.1110.

Ac-L-Ala-Glyco-NHMe (AG). A solution of N-acetyl-L-alanine (0.54 g, 4.2 mmol), the N-methylamide of glycolic acid (0.42 g, 4.7 mmol), and 4-(dimethylamino)pyridine (0.15 g, 1.2 mmol) in THF (13 mL) was cooled to 0 °C, treated with dicyclohexylcarbodiimide (1.2 g, 5.8 mmol), and allowed to warm to room temperature over 12 h. The slurry was suction-filtered, and the filtrate was concentrated. Chromatography (3 vol % MeOH in $CHCl_3$) provided AG as a white powdery solid (0.71 g, 84%): mp 95.5–96.5 °C; R_f 0.38 (10 vol % MeOH in $CHCl_3$); ^1H NMR (200 MHz, $CDCl_3$) δ 7.07 (broad, 1 H), 6.32 (d, J = 7.2 Hz, 1 H), 4.78 (AB q, A part, J = 15.4 Hz, 1 H), 4.55 (AB q, B part, J = 15.4 Hz, 1 H), 4.50 (quintet, J = 7.2 Hz, 1 H), 2.84 (d, J = 4.8 Hz, 3 H), 2.05 (s, 3 H), 1.46 (d, J = 7.2 Hz, 3 H); ^{13}C NMR (67.5 MHz, $CDCl_3$) δ 172.09 (C), 171.34 (C), 167.69 (C), 62.98 (CH_2), 49.05 (CH), 25.90 (CH_3), 22.57 (CH_3), 16.60 (CH_3); IR (1 mM in CH_2Cl_2) 3442, 3360, 1756, 1674, 1671, 1554, 1512 cm^{-1}; EI MS m/e 202.0943, calcd for $C_8H_{14}N_2O_4$ 202.0954.

Ac-^{15}N-L-Ala-Glyc-NHMe (^{15}N-AG). ^{15}N-L-Alanine (0.35 g, 3.9 mmol) was stirred in a solution of acetic anhydride (0.95 mL, 10 mmol) and MeOH (4 mL) for 6 h. Volatiles were removed at a vacuum rotary evaporator, and $CHCl_3$ was added to the resulting light red oil. Upon trituration, Ac-^{15}N-L-Ala-OH was isolated as a white crystalline solid (0.42 g, 82%): ^1H NMR (200 MHz, CD_3CN) δ 6.77 (d, $^3J(^1H^1H)$ = 6.8 Hz; $^1J(^1H^{15}N)$ = 92.4 Hz, 1 H), 4.30 (quintet, $^3J(^1H^1H)$ = 6.8 Hz; d, $^2J(^1H^{15}N)$ = 1.0 Hz, 1 H), 1.90 (d, $^3J(^1H^{15}N)$ = 1.3 Hz, 3 H), 1.32 (d, $^3J(^1H^1H)$ = 6.8 Hz; d, $^3J(^1H^{15}N)$ = 2.9 Hz, 3 H); EI MS m/e 132.0557, calcd for $C_5H_9{}^{15}NO_3$ 132.0553.

A solution of the Ac-^{15}N-L-Ala-OH (0.15 g, 1.1 mmol), the N-methylamide of glycolic acid (0.10 g, 1.1 mmol), and 4-(dimethylamino)pyridine (0.06 g, 0.4 mmol) in THF (5 mL) was cooled to 0 °C, treated with dicyclohexylcarbodiimide (0.29 g, 1.4 mmol), and allowed to warm to room temperature over 6 h. The slurry was suction-filtered, and the filtrate was concentrated. Chromatography (3–5 vol % MeOH in $CHCl_3$) provided ^{15}N-AG as a white powdery solid (0.12 g, 62%): mp 97–98 °C; R_f 0.38 (10 vol % MeOH in $CHCl_3$); ^1H NMR ($CDCl_3$) δ 7.11 (broad, 1 H), 6.43 (d, $^3J(^1H^1H)$ = 6.8 Hz; $^1J(^1H^{15}N)$ = 92.1 Hz, 1 H), 4.78 (AB q, A part, J = 15.3 Hz, 1 H), 4.55 (AB q, B part, J = 15.3 Hz, 1 H), 4.38 (quintet, J = 6.8 Hz, 1 H), 2.84 (d, J = 4.8 Hz, 3 H), 2.05 (d, $^3J(^1H^{15}N)$ = 1.3 Hz, 3 H), 1.46 (d, $^3J(^1H^1H)$ = 6.8 Hz; d, $^3J(^1H^{15}N)$ = 3.1 Hz, 3 H); ^{13}C NMR (67.5 MHz, $CDCl_3$) δ 172.04 (C), 171.23 (C, d, $^1J(^{13}C^{15}N)$ = 13.61 Hz), 167.63 (C), 63.04 (CH_2), 49.04 (CH, d, $^1J(^{13}C^{15}N)$ = 11.88 Hz), 25.89 (CH_3), 22.59 (CH_3, d, $^2J(^{13}C^{15}N)$ = 8.66 Hz), 16.73 (CH_3, d, $^2J(^{13}C^{15}N)$ = 10.23 Hz); IR (1 mM in CH_2Cl_2) 3456 (sh), 3433, 3360, 1756, 1668, 1662, 1557, 1496 cm^{-1}; EI MS m/e 203.0916, calcd for $C_8H_{14}{}^{14}N{}^{15}NO_4$ 203.0924.

Acknowledgment. This work was supported by the National Science Foundation (CHE-9224561). S.H.G. thanks the National Science Foundation Presidential Young Investigator Program (CHE-9157510), the Eastman Kodak Company, Procter & Gamble Company, and Merck Research Laboratories for support. The FT-IR spectrometer was purchased with funds provided by the Office of Naval Research. Departmental computer equipment was purchased with funds from the National Science Foundation (CHE-9007850). We thank Mr. R. Gardner for technical assistance.